VTT PUBLICATIONS 273

Incorporation of model proteins into lipid layers

Aspects of biosensors

Inger Wikholm

VTT Chemical Technology

ACADEMIC DISSERTATION

To be presented, with the permission of the Faculty of Mathematics and Natural Sciences of Åbo Akademi, for public criticism in Auditorium Per Ekwall of the Gadolinia House, Porthansgatan 3 - 5, on May 27th, 1996, at 12 o´clock noon.

Department of Physical Chemistry
Åbo Akademi University
Åbo, Finland

TECHNICAL RESEARCH CENTRE OF FINLAND
ESPOO 1996

ISBN 951-38-4931-7
ISSN 1235-0621

JULKAISIJA – UTGIVARE – PUBLISHER

Valtion teknillinen tutkimuskeskus (VTT), Vuorimiehentie 5, PL 2000, 02044 VTT
puh. vaihde (09) 4561, faksi (09) 456 4374

Statens tekniska forskningscentral (VTT), Bergsmansvägen 5, PB 2000, 02044 VTT
tel. växel (09) 4561, fax (09) 456 4374

Technical Research Centre of Finland (VTT), Vuorimiehentie 5, P.O.Box 2000, FIN–02044 VTT, Finland
phone internat. + 358 9 4561, fax + 358 9 456 4374

VTT Kemiantekniikka, Polymeeri- ja kuitutekniikka, Kanslerinkatu 12 B, PL 14021, 33101 TAMPERE
puh. vaihde (03) 316 3111, faksi (03) 316 3319

VTT Kemiteknik, Polymer- och fiberteknik, Kanslerinkatu 12 B, PB 14021, 33101 TAMMERFORS
tel. växel (03) 316 3111, fax (03) 316 3319

VTT Chemical Technology, Polymer and Fibre Technology, Kanslerinkatu 12 B, P.O.Box 14021,
FIN–33101 TAMPERE, Finland
phone internat. + 358 3 316 3111, fax + 358 3 316 3319

VTT OFFSETPAINO, ESPOO 1996

‘ Ti mamm å papp’

Vikholm, Inger. Incorporation of model proteins into lipid layers. Aspects of biosensors. Espoo 1996, Technocal Research Centre of Finland, VTT Publications 273. 53 p. + app. 65 p.

UDC 663.1:681.586:577.112

Keywords Langmuir-Blodgett films, layers, immobilization, proteins, antibodies, biosensors, detectors, surface acoustic wave device, quartz crystal microbalance, surface plasmon resonance, atomic force microscopy, lipids

ABSTRACT

In this work different approaches of the Langmuir-Blodgett (LB) technique have been studied in order to obtain an oriented and sensitive protein layer onto a solid surface. LB films of Cd arachidate or self-assembled films of octadecylmercaptan have been used as supports for the artificial protein layers. It is essential that the support is defect-free in order to minimise non-specific binding.

The quality of LB layers of Cd arachidate was noticed to be strongly influenced by how the solid slide was positioned in relation to the compressing barrier during vertical deposition. Atomic force microscopy, AFM, revealed that the layers were more homogeneous, if the slide was placed parallel to the compressing barrier. The amount of layer transferred could be determined by using either a surface acoustic wave device or a quartz crystal as a microbalance. Moreover, surface plasmon resonance, SPR, could be used to evaluate monolayer transfer.

Unilamellar vesicles fused to form monolayers when spread onto the air-water interface. The layers could be transferred to hydrophobic supports as visualised by AFM. This could be a means to incorporate membrane proteins into lipid layers, as membrane proteins easily can be embedded into vesicles. Aged vesicles were transferred as large domains.

Antibodies of the C-reactive protein, CRP, formed a monolayer, when spread directly onto the air-water interface. The antibodies seemed to take up a slanted orientation or have a random distribution in the monolayer. Antibodies were also adsorbed from the subphase onto various monolayers. Binding of anti-CRP was dependent on the packing of the film, on the antibody concentration in the aqueous subphase, but also on the monolayer matrix. The binding was highest to a monolayer of octadecylamine. The monolayer was, furthermore, stabilised by the antibodies. Evaluation of the specific interaction between the antigen-antibody complex with a quartz crystal microbalance indicated that the antigen could be determined in the concentration range of 0.1 - 5 µg/ml.

In order to obtain site-directed immobilization, various amounts of a biosynthetically produced lipid-tagged single-chain antibody were incorporated into phospholipid monolayers preformed at the air-water interface. Incorporation of the single-chain antibodies, transfer of the layer onto solid slides, amount of non-specific adsorption and thus the amount of specific binding depended on the composition of the lipid matrix. Studies by AFM revealed that the film consisted of antibody-enriched lipid domains and that the films were not stable when stored long times in aqueous solution. The binding of hapten, which was used as an antigen, could be detected with SPR in the concentration range of 0.1 - 100 µg/ml.

PREFACE

This work has been carried out at the Technical Research Centre of Finland (VTT) in the Chemical Sensor Group of Chemical Technology (earlier part of the Medical Engineering Laboratory) during the years 1989-1995.

I am very grateful to my research manager Dr. Antero Aspiala and my former laboratory director Professor Niilo Saranummi for providing the working facilities and giving me the opportunity to work with my thesis at VTT.

I am indebted to Professor Jarl B. Rosenholm for allowing me to present my dissertation at the Department of Physical Chemistry at Åbo Akademi University.

I want to express my warmest appreciation to my colleagues in the Chemical Sensor Group; to our group manager Doc. Jukka Lekkala for an encouraging attitude towards my work and to Hannu Helle MSc, Jyrki Kimmel TechLic, Doc. Janusz Sadowski, Martin Albers BSc, Harri Joki MSc and Pekka Lumme Tech for creating a pleasant working atmosphere. Furthermore, I would like to thank Jarmo Kylä-Laurila and Risto Poramo for skilful assistance in solving some of the technical problems.

I would like to extend my appreciation to Prof. Olle Teleman for valuable critical advice on my work. I also want to thank Dr. Jouko Peltonen and Erika Györvary TechLic for a fruitful collaboration.

Finally, I warmly thank Mikael, my parents, Sven and Hjördis, and my dear brothers Bo and Bror for showing interest in my studies all these years.

Financial support from the Academy of Finland is gratefully acknowledged.

Inger Vikholm
Tampere, April 1996

CONTENTS

Appendices of this publication are not included in the PDF version. Please order the printed version to get the complete publication (http://www.inf.vtt.fi/pdf/publications/1996)

LIST OF PUBLICATIONS

This dissertation is based on the following scientific papers, which are referred to in the text by their Roman numbers. Some unpublished results are also presented.

I Characterization of N,N'-diarachidoyl indigo transferred onto a surface acoustic wave device.
Vikholm, I. and Helle, H.
Thin Solid Films 178 (1989) 197 - 202.

II Langmuir-Blodgett film deposition studied by a surface acoustic wave device.
Vikholm, I. and Helle, H.
Progress in Colloid and Polymer Science 81 (1990) 163 - 165.

III Biosensors based on surface plasmons excited in non-noble metals.
Sadowski, J., Lekkala, J. and Vikholm, I.
Biosensors and Bioelectronics 6 (1991) 439 - 444.

IV Adsorption of antibodies to a Langmuir layer of octadecylamine and the interaction with antigen.
Vikholm, I. and Teleman, O.
Journal of Colloid and Interface Science 168 (1994) 125 - 129.

V Atomic force microscope images of lipid layers spread from vesicle suspensions.
Vikholm, I., Peltonen, J. and Teleman, O.
Biochimica et Biophysica Acta 1233 (1995) 111 - 117.

VI Layer formation of a lipid-tagged single-chain antibody and the interaction with antigen.
Vikholm, I. and Peltonen, J.
Thin Solid Films, Accepted for publication, 10 p.

VII Incorporation of lipid-tagged single-chain antibodies into lipid monolayers and the interaction with antigen.
Vikholm, I., Györvary, E. and Peltonen, J.
Langmuir, Accepted for publication, 26 p.

The contribution of the author has been the following:

In Papers I and II, the derivation of an indigo dye with two hydrophobic chains was done by my colleague Hannu Helle MSc, whereas I was in charge of the studies on the LB film formation.

In Paper III, my colleagues Doc. Janusz Sadowski and Doc. Jukka Lekkala were responsible for the surface plasmon resonance modelling and measurements, whereas I transferred LB films onto the metallic slides.

The experimental work in Paper IV was done entirely by myself. Prof. Olle Teleman made some valuable critical comments on manuscripts IV and V.

In Papers V and VI, the atomic force microscopy measurements were done by Dr. Jouko Peltonen and in Paper VII, by Erika Györvary TechLic at Åbo Akademi University. The monolayer formation, deposition, quartz crystal microbalance and surface plasmon resonance studies were done by myself.

I have been in main charge of the preparation of Papers I, II and IV-VII.

LIST OF SYMBOLS

A	molecular surface area, $Å^2$/molecule
Au	gold
AFM	atomic force microscopy
ALDH	aldose dehydrogenase
BSA	bovine serum albumin
CHOL	cholesterol
CRP	C-reactive protein
C_{20}	arachidic acid
C22	behenic acid
DMPC	dimyristoylphosphatidylcholine
DMPE	dimyristoylphosphatidylethanolamine
DPPA	dipalmitoylphosphatidic acid
DPPC	dipalmitoylphosphatidylcholine
DPPE	dipalmitoylphosphatidylethanolamine
*f*o	resonant frequency of the device, Hz
IgG	immunoglobulin G
kD	kilodalton
LB	Langmuir-Blodgett
lpp	the major lipoprotein of *Escherichia coli*
M	average molar mass of substance, g/mol or kD
ODA	octadecylamine
Ox	2-phenyloxazolone
Ox_{16}BSA	BSA containing 16 molecules of Ox
Pd	palladium
SAW	surface acoustic wave
scFv	single-chain antibody
SPR	surface plasmon resonance
QCM	quartz crystal microbalance

δ	change in
Λ	surface mass density, $\mu g/cm^2$
Π	surface pressure, mN/m
τ	transfer ratio

1 INTRODUCTION

There is an increasing need for simple, rapid, and easy-to-use biosensors for use in emergency units, doctor's offices or even at home to aid clinical diagnosis. Antibody-antigen complex formation is very specific and used to measure the concentration of antigen. This determination can be important for diagnosis because the antigens can be viruses or bacteria that are involved in such illnesses as cancer and AIDS. Interactions between antibodies and antigens have traditionally been measured using, for example, radio immunoassay, solid phase enzyme immunoassay or fluorescence quenching techniques [1]. All these approaches rely on a marker molecule, such as a radioisotope, an enzyme or a fluorescent probe, that amplifies and allows quantification of the antibody-antigen interaction. Mostly, the result is not obtained until several incubations, washing and separation steps have taken place. A future prospective is to develop a biosensor, that can monitor antigen concentrations in real-time with the aid of an immobilized antibody.

A biosensor is built up of a molecular recognition site, in which a change occurs upon entrapment of a specific substance (Fig. 1). The chemical or physical change is detected and transduced into electronic or optical signals by modern electronic devices; transducers. The recognition site can be made up of an enzyme, that shows specific catalytic activity towards its substrate, or an antibody with molecular recognition activity toward an antigen. Biosensors are designed to be simple, selective, rapid and accurate.

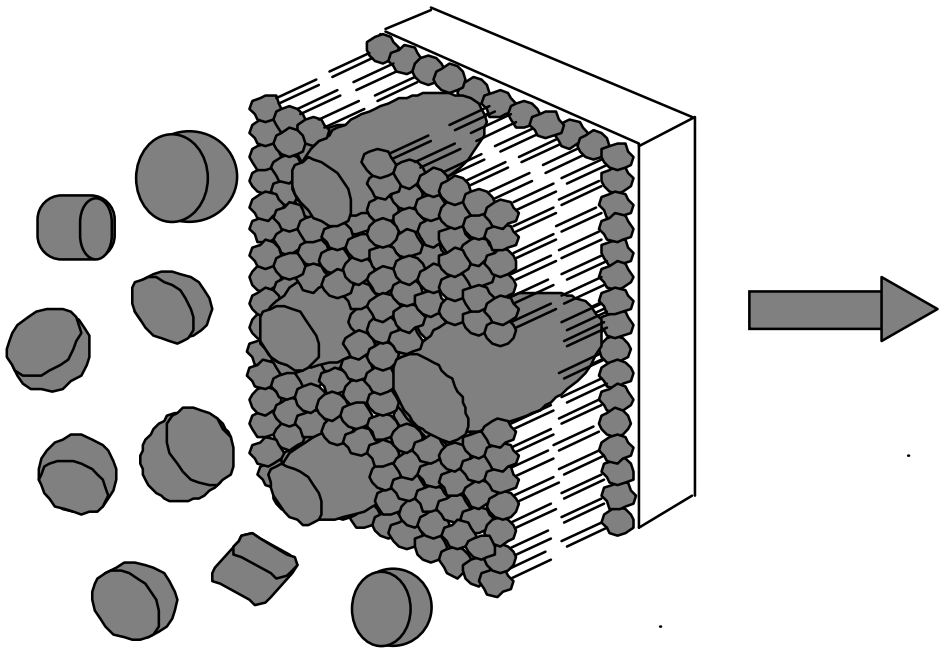

Figure 1. Schematic view of a biosensor.

The main challenge in biosensor technology today is the ability to attach biomolecules to the transducer so that they are anchored with their activity and specificity intact. Neither of the most commonly used techniques for protein immobilization have been able to achieve a monolayer of receptor molecules reliably coupled to a solid support. Covalent bonding achieves the most stable attachment, but there are restrictions in the degrees of freedom, cross-linking causes a partial loss in activity, adsorption gives an unstable attachment and entrapment in a gel network is prone to release of protein through the network [2-4]. Moreover, there are problems with these methods concerning reproducibility, non-homogeneity and orientation of the biomolecules. The Langmuir-Blodgett (LB) technique has recently been employed to solve some of these problems.

This thesis is concentrated on research relevant to biosensors. Different approaches of the LB technique have been studied in order to obtain a homogeneous, oriented, stable, reproducible and sensitive layer of proteins onto the sensor surface [IV-VII]. Proteins have been incorporated into monolayers with emphasis on mimicing the membrane of a living cell with proteins intercalated among lipid molecules as shown in Fig. 1. LB layers of fatty acids have been studied as hydrophobic supports for the artificial protein layer [I-III, V].

The outline of this thesis is as follows. The layer formation of both amphiphilic molecules and proteins are presented as well as the methods used for characterization. Some characteristics of the materials studied are also included. The most important experimental results on the transferability and homogeneity of LB layers are briefly discussed, while the monolayer-forming properties of the proteins and the functional activity of these layers are discussed in more detail.

2 METHODS

The LB technique has been well described in the literature and only a brief introduction will be given here [5-8]. The methods used for characterization of the layers will, on the other hand, be discussed in more detail.

2.1 LAYER FORMATION AND DEPOSITION OF AMPHIPHILIC MOLECULES

Amphiphilic molecules possessing a hydrophilic head group and a long hydrophobic alkyl chain are classic monolayer-forming materials. When these molecules are dissolved in a water-immiscible solvent and placed on a water surface they are rapidly spread to cover the available area. The molecules can be compressed to a monolayer when the solvent has evaporated. The monolayer-forming properties can be governed by plotting the surface pressure as a function of the surface area available for the molecules. When the distance between the molecules is large, their interactions are small, and they can be regarded as forming a two-dimensional gas. As the area is reduced the molecules exert a repulsive effect on each other and depending on the amphiphilic nature of the molecules a monolayer is formed. If the available surface area becomes too small the monolayer collapses. Molecules that do not have an appropriate amphiphilic nature are often incorporated into monolayers by mixing with carboxylic acids [6-8, I, II]. The area of these molecules can be calculated if they are mixed with each other at a molecular level [I].

Insoluble monolayers of amphiphilic molecules exhibit surface pressure relaxation at a constant area or area relaxation at a constant surface pressure [9]. Maximum monolayer stability of carboxylic acids and amines occurs when the film is roughly half-ionised [9]. The stability of the monolayer at the air-water interface is of utmost importance when transferring the layer onto a solid slide [10].

Monolayers can be built up on a solid slide oriented normal to the monolayer, by passing the slide through the monolayer-water interface while the surface pressure is maintained constant (Fig. 2a) - the classical vertical method by Langmuir and Blodgett [5]. Multilayers mostly take up a bilayer structure, they are Y-type, but monolayers can also be transferred only when the slide is inserted into the subphase or only when it is withdrawn (X- and Z-type deposition). The transfer ratio, τ, defined as the ratio of the area of monolayer removed from the water surface to the area of the slide coated by the monolayer, is often used to measure the quantity of deposition [8].

X-type monolayers can also be transferred by bringing the slide horizontally into contact with a monolayer that is surrounded by a frame (Fig. 2b), and lifting the slide up at a small angle [11-13]. Recently, it has been shown that Y-type monolayers can be transferred horizontally, if the monolayer is not surrounded by a frame [14].

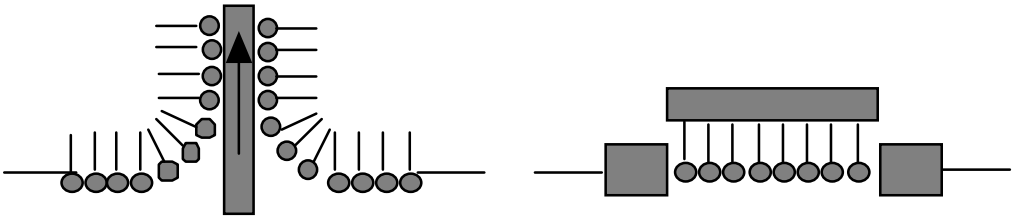

a) b)

Figure 2. Monolayer transfer onto solid slides by a) vertical and b) horizontal deposition.

2.2 PROTEIN LAYERS

The general concept of a biomembrane consists of a bilayer composed of a variety of amphiphilic molecules, mainly phospholipids and sterols into which membrane proteins are embedded via hydrophobic and electrostatic interactions [15,16]. Proteins can also be found attached to the surface of the bilayer. Various approaches can be employed to construct a biological membrane by the LB technique [8]. First of all, a monolayer must be prepared at the air-water interface. In this thesis four methods were studied:

1. Vesicles were fused onto the air-water interface in order to embed a membrane protein into lipid monolayers [V],

2. antibodies were spread directly onto the air-water interface [IV] or

3. adsorbed from the subphase onto various monolayers [IV], and

4. a lipid-tagged single-chain antibody was incorporated into monolayer matrices by spreading from a detergent solution [VI, VII].

LB layers of fatty acids or a self-assembled layer formed the hydrophobic support onto which the protein layers were transferred. A description of the experimental details can be found in the individual publications. The preparation of vesicles will, however, be described below. Moreover, a general outline of work related to the methods will be given.

2.2.1 Preparation of vesicles

Phospholipids may be caused to aggregate in solution to form sub-microscopic, spherical bilamellar structures called vesicles. Vesicles may be unilamellar, composed of only one bilayer or multilamellar having a plurality of compartments, depending on the preparation methods used. Sonication is the most simple way to produce unilamellar vesicles [17]. The research on vesicles ranges from membrane reconstitution studies to their use for answering questions in cell biology and therapeutics, where vesicles can serve as a carrier vehicle to introduce biologically active materials into cells or into the cell wall [17].

In this work small amounts of unilamellar vesicles have been prepared by sonication in a bath ultrasonic disintegrator. The vesicles were used as freshly prepared and have been referred to as fresh vesicles [V]. Vesicles have also been prepared by probe sonication. Varying amounts of a purified membrane protein were incorporated into these vesicles and the suspensions were stored at 253 K until used, to avoid denaturation of the protein [18]. These vesicle suspensions were kindly obtained from the Biotechnology and Food Research of the Technical Research Centre of Finland and have been referred to as aged vesicles [V].

Sonicated vesicles can vary in size and they are, furthermore, unstable with respect to the gradual growth of large vesicles at the expense of smaller ones, because of the bending energy associated with the bilayer curvature [19]. In order to get better control over the size of the vesicles an injection method giving unilamellar vesicles with a diameter of about 100 nm [20] have later on been taken into practice. The work related to these vesicles will, however, not be discussed in this thesis.

2.2.2 Layer formation by fusion of vesicles

The original work of spreading vesicles onto the air-water interface was performed by Verger et al. [21], who spread brush border membrane vesicles along a wet glass rod. The vesicles opened and their internal content was released into the aqueous subphase. Various methods have since been used, but the results are controversial. Some workers claim to obtain a monolayer [22-28], while others find non-homogeneous bilayers or more complex structures [29-31]. Fusion of vesicles has been proposed to occur through defects in the vesicle outer monolayer [32]. The spreading of vesicles directly onto solid supports [32] and the procedure for separating the vesicle suspension and the monolayer at the air-water interface by using a wet bridge will not be discussed in this thesis [26].

2.2.3 Layer formation of proteins at the air-water interface

The preparation and nature of protein films at the air-water interface have been the subject of continued investigation [33, 34]. Studies on the spreading of antibodies are limited [35-40]. It is believed that proteins that are spread at the air-water interface at a surface concentration below 1mg/m^2 are denaturated at the interface through disruption and unfolding of the tertiary structure [34]. When concentrations above 1mg/m^2 are spread retention in activity is thought to be explained by incomplete unfolding. The ability to retain some level of activity is, however, dependent on the specific protein [34].

2.2.4 Adsorption of proteins onto a preformed monolayer

The adsorption of various biomolecules from solution to a preformed monolayer at the air-water interface has been studied by several groups [41-59]. Proteins can be adsorbed from the subphase onto a monolayer by both hydrophobic and electrostatic interactions. Small protein molecules penetrate into the monolayer at low surface pressure, whereas bigger ones only adsorb onto the monolayer [47]. Most studies have been carried out on enzymes [48-51], but recently studies have also been performed on the binding of streptavidin and avidin from the subphase to a preformed biotinylated lipid layer [52-55]. Some groups have, moreover, reported on the adsorption of antibodies [56-59].

2.3 CHARACTERIZATION

Mass sensitive methods and the optical method based on SPR have recently attracted great interest as measuring techniques for biosensors, because they can offer direct measurement, simplicity, small sensor size and low cost [60-65].

2.3.1 The quartz crystal microbalance

The principle of the QCM is based on a change in the resonance frequency of the crystal due to an alteration of mass on its surface. The decrease in frequency, δf (Hz) upon deposition of material can be converted to a change in mass per unit area, $\delta m/A$ (g/cm^2) according to Sauerbrey´s equation [61]:

$$\delta f = - \frac{2 f_o^2 \, \delta m/A}{\rho_q \upsilon_q} \qquad [1]$$

where f_o (Hz) is the resonance frequency, ρ_q is the density and υ_q is the shear wave velocity for AT-cut quartz. The QCM has been used as a sensitive mass [61] and viscosity monitoring device [62]. A large number of analytical applications in the area of gas sensing, trace ion determination and immunoassay [63,64] have been published.

The 10 MHz AT-cut quartz crystal used in this work was obtained from Universal Sensors Inc. The QCM was connected to a custom-built oscillator and driven at 5 Vdc. The frequency of the vibrating crystal was measured by a universal frequency counter (HP 5316B). The QCM did not resonate in liquid and was mainly used to evaluate the horizontal transfer of layers [IV-VII] and to monitor the adsorption of protein [IV].

2.3.2 The surface acoustic wave device

A detailed description of the design and operation of SAW devices can be found in the works of Wohltjen [66,67]. Briefly, a SAW device consists of a quartz wafer with sputtered interdigital metal electrodes. A mechanical Rayleigh wave propagates across the surface between transmitter and receiver electrodes, when the former is excited by a radio frequency (RF) voltage. The device starts to oscillate at the frequency determined by the interdigital-electrode-spacing and the Rayleigh-wave velocity, when the electrode pair is connected through a RF-amplifier. Deposition of material on the device leads to a substantial reduction of the Rayleigh-wave velocity and a corresponding decrease in the resonant frequency. The shift in frequency, δf (Hz), can be calculated as a change in mass per unit area, $\delta m/A$ (kg/m^2) according to:

$$\delta f = (k_1 + k_2)\, f_o^2\ \delta m/A \qquad [2]$$

where f_o (Hz) is the resonant frequency of the device, and k_1 and k_2 are material constants [66]. The sensitivity of piezoelectric devices is directly proportional to the square of the resonant frequency, and inversely proportional to the surface area as seen from Equation 1 and 2. SAW devices resonate at a much higher frequency than the QCM. The use of SAW devices for sensing chemical vapours was first reported by Wohltjen et al. [67] and has since been investigated by several other groups [68,69].

A 77.8 MHz SAW device manufactured by Vaisala Oy (Helsinki, Finland) was used in this work to monitor water entrainment and to evaluate the transferability of LB layers [I, II]. The change in frequency was measured each time the device was raised out of the monolayer-water interface.

2.3.3 Surface plasmon resonance

A surface plasmon is an electromagnetic wave propagating along the surface of a thin metal layer. When monochromatic, p-polarised light undergoes total internal reflection at a glass-dielectric interface, an evanescent electromagnetic field is created. If a thin metallic film is placed onto the glass (the so-called Kretchmann configuration) the electromagnetic field polarised parallel to the incident plane excites collective oscillations of free electrons within the metal (Fig. 3a). This field has maxima at the metal-dielectric boundaries and dies away exponentially in the direction perpendicular to the interface (Fig. 3c). Surface plasmons are therefore sensitive to dielectric permittivity changes near the metal-dielectric interface. Surface plasmon resonance, SPR, is observed as a sharp minimum in the intensity of the reflected light at a specific angle of the incident light, the resonance angle (Fig. 3b) [65,70,71].

The properties of the SPR curve depend on the wavelength and polarisation state of the incident light, on the optical constants - the refractive index, the extinction coefficient and the thickness - of the glass support and the metal film and on the optical properties of the dielectric medium interfacing with the non-illuminated side of the metal film. Any surface modification in the immediate vicinity of the metal, such as a lipid layer, will change the resonance conditions by shifting the position of the reflection minimum and altering the shape of the resonance curve. The shape of the SPR curve can be quantitatively described by Fresnel´s equations [III]. A more extensive theoretical description of SPR is given in Paper III.

The experimental apparatus used in these studies is shown in Fig. 3a and has been described by Sadowski et al. [72]. Briefly, a beam of light from a 10 mW He-Ne laser (λ=632.8 nm, polarized output) was divided into two parts by a beamsplitter and one of the beams was passed through a glass prism onto the back surface of a metallic film. The metal had been e-beam evaporated onto BK-7 glass slides and sealed to the prism with an index-matching oil. The prism was fixed on a rotating table and the table was driven by a stepper motor, with one step corresponding to a degree of 0.01. The intensity of the light reflected from the prism and that of the reference beam was measured by solid state detectors, amplified by lock-in amplifiers, digitized by an analog-to-digital converter and recorded by a personal computer.

The SPR resonance curve was determined by recording the reflected light intensity as a function of the angle of incidence by turning the prism against the laser beam. Moreover, computer simulations based on Fresnel´s equations were used in Paper III to numerically predict the behaviour of the SPR curve coated with different number of layers. The optical sensitivity of the apparatus depends on the metal used and is in the range of $dn=10^{-6}$ for samples exposed to air, and $dn=10^{-5}$ for liquid samples [73].

During the immunological measurements a liquid cell was placed over the measurement area of the coated Au slide and was filled with buffer. When the SPR resonance curve of the film in contact with liquid had been recorded (Fig.3b), the angle of incidence was driven to a point slightly above the resonance minimum. Changes in the intensity of the light at this angle were detected as protein was injected into the cell [VI, VII]. At the end of each series of measurement the cell was rinsed with buffer and the SPR resonance curve was recorded once more.

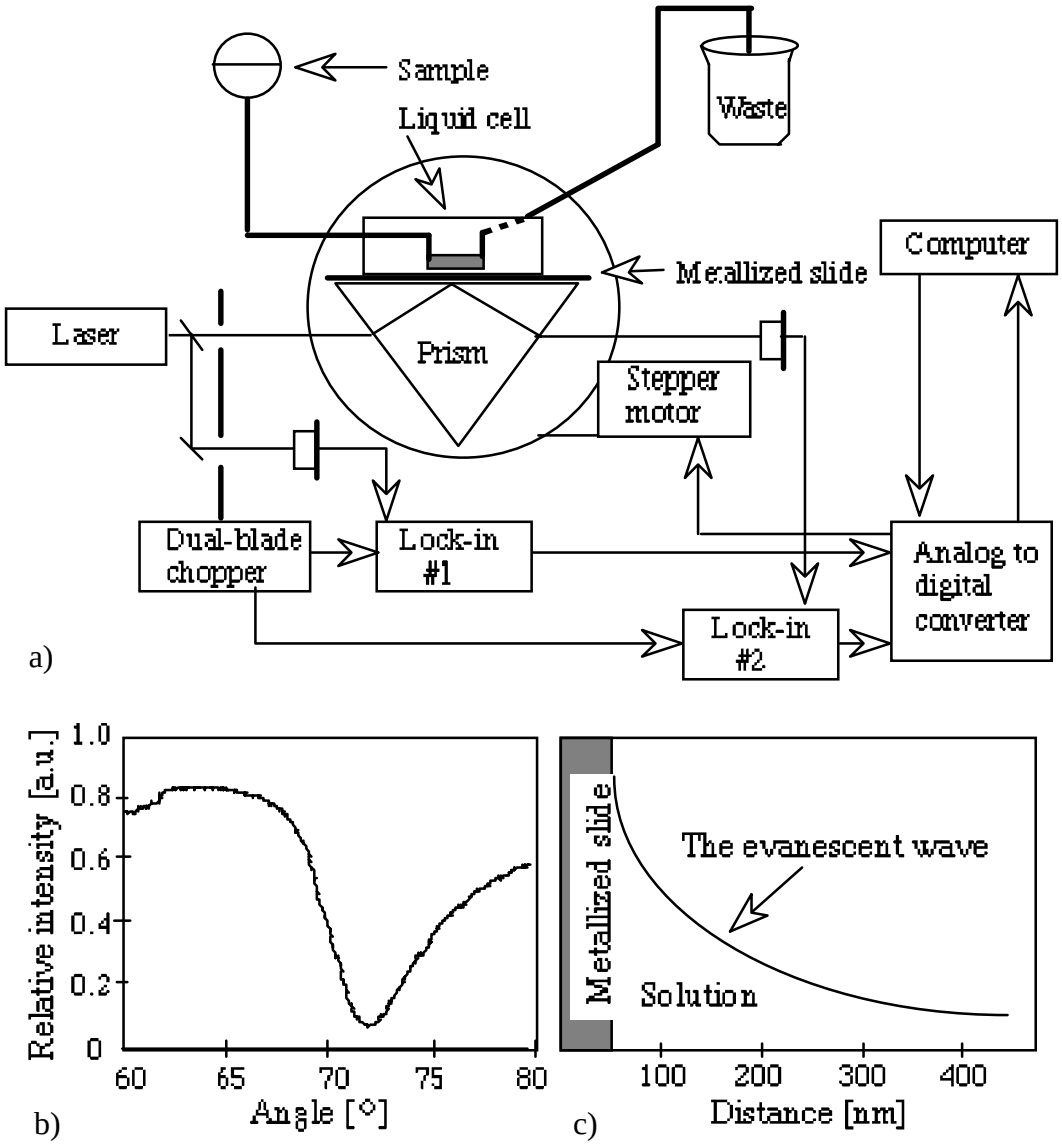

Figure 3. a) A schematic view of the SPR set-up. The liquid cell has a diameter of 4 mm and a depth of 0.6 mm. b) SPR is observed as a sharp dip in the reflectance with respect to the incident angle. c) The intensity of the evanescent wave decreases exponentally with the distance from the metal-solution interface.

SPR has been successfully used to investigate the optical properties of a range of metal films, to characterize LB multilayers [III, 74,75] and to monitor biotin/streptavidin binding and the subsequent binding of biotinylated antibodies and antigens [76].

2.3.4 Surface imaging with atomic force microscopy

AFM has emerged as an important tool for imaging thin films at molecular resolution in both air and liquid environments [77-81]. A sharp tip is mounted on a cantilever arm and scanned across a sample surface (Fig. 4a). AFM images are obtained by recording the force acting between the tip and the sample. A light beam of a laser diode is focused onto the end of the cantilever. Bending and torsion of the cantilever changes the reflection of the laser beam. Topographic imaging is obtained by recording the vertical deflection of the cantilever. In conventional AFM the angular deflection of the light is measured with a two-segment photo diode. The difference in intensity of the reflected light is fed as signals into a feedback circuit that control the z motion of an xyz translator. The feedback between the photo diode and the z-piezo enables imaging in two modes; in the constant-force mode the photo diode signal (i.e. the tip deflection) is kept constant by tuning the sample height position with the z-piezo, and in the constant-height mode, the sample height is kept unchanged and the fluctuations in the cantilever deflection give the image contrast during scanning with the x- and y-piezos [87]. In addition to topographical imaging, AFM can be used to measure frictional interaction between the tip and the sample [79,82-85]. An image of the friction forces is obtained by monitoring the deflection of the cantilever constrained to lateral movement by using a four-segment photo diode (Fig. 4a).

Fig. 4b shows a typical AFM force-distance curve carried out by monitoring the deflection of light off the back of the cantilever as the sample is approached or withdrawn from the tip by an xyz translator. There is no interaction when the tip and the sample are well separated (non-contact line). The sample is moved against the cantilever till the sample comes so close that the cantilever deflects. Here there are a variety of complex attractive and repulsive interactions that contain the majority of information about the interactions between the tip and the sample [83]. After contact the tip and sample movements are linearly coupled in the contact line. Hysteresis is often exhibited between the approaching and withdrawing portions of the contact line. Finally, the tip jumps off the sample surface, when the withdrawal of the sample is continued.

The resolution of the AFM is limited by the finite sharpness of the probing tip [86]. In fact the AFM tip distorts the size of globular domains so that their real diameters appear increased. The real diameter, d, of the domains can be estimated according to $d = l^2 / 8 \cdot R$, where l corresponds to the measured diameter of the domains and R is the radius of curvature of the tip [87].

A Nanoscope II-AFM (Digital Instruments Inc.) was used for sample surface imaging in air [V, VI] and a Nanoscope III-AFM equipped with a four-quadrant photo diode enabled simultaneous probing of friction and topography in liquid conditions [VII]. All images were acquired in the constant force mode. The AFM tips used in this work were assumed to be rounded, with a curvature radius of about 50 nm [88]. The experimental details are given in the related papers [V-VII].

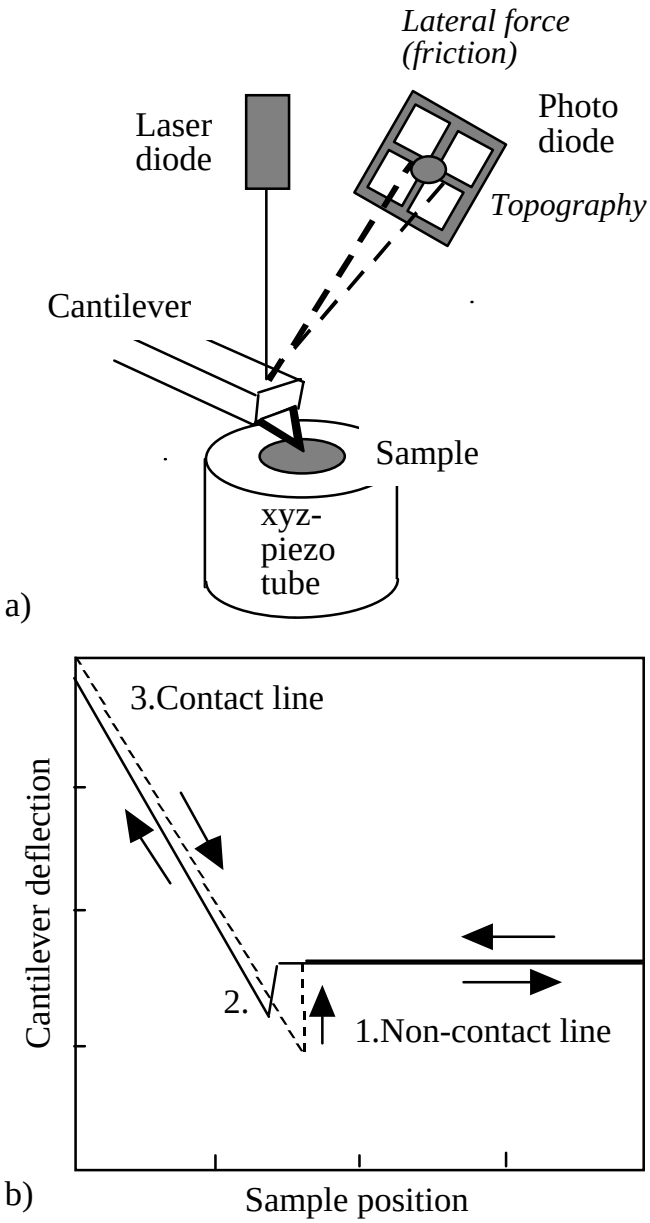

Figure 4 a) Schematic view of the atomic force microscope imaging topography and friction with light reflected onto a four-segment photo diode and b) a typical force versus sample position curve. The point of contact or near contact between the sample and the tip is indicated by 2.

3 MATERIALS

3.1 AMPHIPHILIC MOLECULES USED FOR FILM FORMATION

The amphiphilic molecules used for LB-layer formation were carboxylic acids, an alkyl amine and phospholipids. The molecules are listed in Table 1 and the molecular structure of some of the amphiphiles is shown in Fig. 5. Phospholipids and particularly phosphatidylcholines are major constituents of cell membranes and it is generally accepted that all biomembranes are built upon a lipid matrix in which proteins are embedded [15,16]. Both synthetic and naturally occurring lipids have been used as simple models of biological membranes [89]. The monolayer-forming properties of 1,1´-diarachidoylindigo are not of great interest in this context and will not be discussed [I, II].

Table 1. Amphiphilic molecules used for LB layer formation.

Name	Abbr.	M [g/mol]
Arachidic acid	C_{20}	312.5
Behenic acid	C_{22}	340.6
Octadecylamine	ODA	269.5
1,2-dimyristoylphosphatidylcholine	DMPC	677.9
1,2-dipalmitoylphosphatidylcholine	DPPC	752.1
1,2-dimyristoylphosphatidylethanolamine	DMPE	635.9
1,2-dipalmitoylphosphatidylethanolamine	DPPE	692.0
1,2-dipalmitoylphosphatidic acid	DPPA	648.9
Cholesterol	CHOL	386.9

The gold slides used during SPR measurements as supports for the protein films were rendered hydrophobic by a self-assembled monolayer of 1-octadecanethiol [VI, VII]. Alkanethiols and dialkyl disulphides bind to gold surfaces via a gold tiolate to form ordered, oriented monolayers. Self-assembled layers are well documented in the literature [90,91] and will not be discussed in this thesis.

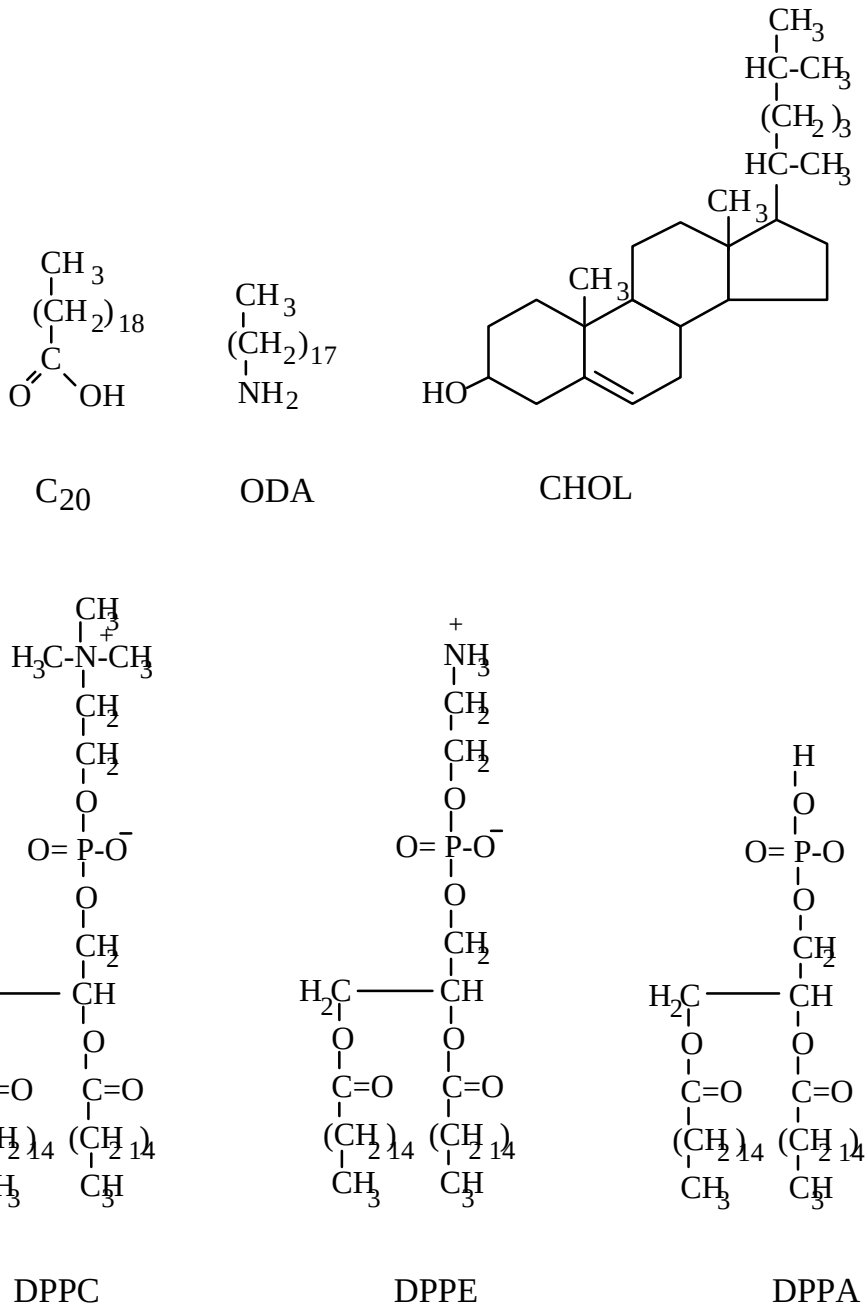

Figure 5. Chemical structures of some of the studied molecules.

3.2 GENERAL ASPECTS OF ANTIBODIES

Antibodies or immunoglobulins (Ig) appear in the blood serum and certain cells in response to the introduction of a protein or some other foreign macromolecule, an antigen. The antibodies are specific and can combine with the antigen to form an antigen-antibody complex. Antibody molecules are essentially required to recognize and bind the antigen, and to trigger the elimination of foreign material.

A human is capable of producing antibodies against more than 10^6 different molecular structures.

Antibodies are large proteins with a Y-shaped structure consisting of four polypeptide chains, two identical heavy (H) chains (50 kD) and two identical light (L) chains (25 kD). A single disulphide bond connects light and heavy chains and a variable number connects the two heavy chains. The light and heavy polypeptide chains are folded into globular regions called domains (Fig.6). The portion between the domains of the heavy chains known as the hinge region can be cleaved by proteolytic enzymes, dividing the antibody structure into three units. Two of the units are identical and involved in the binding to antigen - the Fab (antigen-binding fragment) arms of the molecule. The Fv (variable) fragment on the tip of each arm confers on the antibody its unique antigen-binding specificity. These fragments contain the variable light (V_L) and variable heavy (V_H) domains, which vary greatly from one antibody to another. Stable Fv fragments can be engineered by linking the domains with a peptide to create single-chain Fv fragments (scFv). The third unit, Fc (fragment crystalline), is responsible for triggering effector functions that eliminate the antigen [92,93].

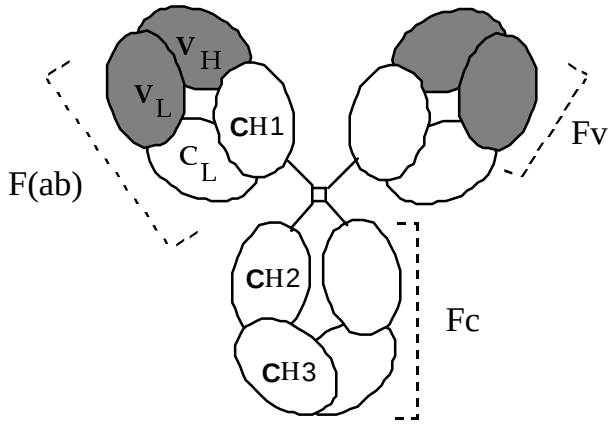

Figure 6. γ-immunoglobulin IgG is a Y-shaped molecule composed of four polypeptide chains linked by disulphide bonds. The light chains are folded into two domains, V_L (variable) and C_L (constant), while the heavy chains consist of V_H, C_H1-C_H3 domains. The Fab units are identical and carry on the tip of each arm the variable regions - the Fv fragment capable of binding antigen.

3.3 MODEL PROTEINS

Monolayer formation and incorporation of enzymes into Langmuir layers have been extensively studied. The interest of my studies was therefore mainly focused on the immobilization of antibodies. The studied model proteins are listed in

Table 2. Bovine serum albumin, BSA, a water-soluble blood protein, was used to block non-specific binding sites, whereas the C-reactive protein, CRP, and the hapten, Ox_{16}BSA, were used as antigens [IV, VI, VII].

Table 2. Model proteins used for monolayer formation and proteins used in the adsorption studies.

Name		M [kD]
anti-C-reactive protein	anti-CRP	160
lipid-tagged anti-2-phenyloxazolone single-chain IgG1	Ox lpp-scFv	28
aldose dehydrogenase	ALDH	80
C-reactive protein	CRP	120-140
2-phenyloxazolone-BSA	Ox_{16}BSA	70
bovine serum albumin	BSA	67

CRP and immunoglobulin G have a similar amino acid sequence [94, 95]. CRP is composed of five identical non-covalently linked subunits arranged as a regular pentagon [95,96]. Detection of CRP is of interest because raised concentrations of CRP may be a result of many immunological reactions and inflammatory processes [97]. CRP increases from normal values less than 1 mg/l to as much as several hundred mg/l in response to most forms of tissue injury, inflammation or infection.

Single-chain antibodies of anti-2-phenyloxazolone IgG1 have been expressed and secreted in *Escherichia coli*, joined together by a short peptide and fused with the major lipoprotein of *E. coli* [98]. This lipid-tagged antibody fragment, designed as Ox lpp-scFv, can be solubilized with non-ionic detergents and incorporated into vesicles with remaining functional activity [99].

Aldose dehydrogenase (ALDH) from *Gluconobacter oxydans* was chosen as a model protein, because of its membrane-binding properties. ALDH has five hydrophobic regions probably forming the anchor, that attaches the enzyme to the membrane. The rest of the enzyme is water soluble. Hence, it could be expected that part of the enzyme would be buried in the hydrophobic moiety and the other part would be in contact with the aqueous environment [18]. ALDH is most sensitive to glucose, but shows response also to xylose, galactose and arabinose [18].

4 RESULTS AND DISCUSSION

4.1 SOME ASPECTS OF MONOLAYER TRANSFER

4.1.1 Surface density monitoring with mass sensitive resonators

The transfer ratio is generally used to estimate the deposition of monolayers onto solid supports. The mass of the transferred layers can, however, easily be measured with a QCM [100, IV-VII] and with a SAW device [I, II]. The change in frequency versus number of layers gives additional information about the transfer. The existence of a negative intercept suggests that the first layer packed more loosely than the subsequent layers [I, II]. The increase in frequency after deposition, furthermore, indicated that water molecules are transferred with the polar head groups of CdC_{20} during deposition [II]. The layers therefore have to be dried before successive deposition [II]. This can, however, lead to holes and cracks in the film.

The transfer ratio can also be obtained as a ratio between measured and expected surface mass densities (Table 3 and Fig.7). The deviation in transfer ratio from unity on deposition of CdC_{20} indicates that the packing of the molecules differed from that in the Langmuir layer (Fig.7). The perpendicular orientation of the SAW device in relation to the compressing barrier during vertical deposition influenced the surface density of the layers, as will be discussed later [V]. It is also possible that the surface acoustic waves were attenuated because of a scattering from defects in the layer. Horizontal deposition gave a lower transfer ratio than vertical deposition, which is consistent with the AFM images that showed a difference in the uniformity of the film [V].

Table 3. Comparison of measured and expected resonator surface mass densities, $\delta\Lambda^*$ and $\delta\Lambda^{**}$*, sensitivity,* $\delta f/\delta\Lambda$ *and transfer ratio on deposition of LB layers.*

Device	δf [Hz]	$\delta\Lambda^*$ [μg/cm^2]	$\delta\Lambda^{**}$	$\delta f/\delta\Lambda^*$ [Hz cm^2/ng]		τ
78 MHz SAW	2400	0.290	0.307	8.3	0.945	[CdC_{20}, I]
10 MHz QCM	55	0.239	0.307	0.23	0.777	[CdC_{20}]
10 MHz QCM	44	0.190	0.220	0.23	0.864	[DMPC, V]

The layers were vertically transferred onto the SAW device and horizontally transferred onto the QCM.

The SAW device appears to be more attractive than the QCM, because of a higher mass sensitivity (Table 3). A low noise level, however, speaks in favour of the QCM.

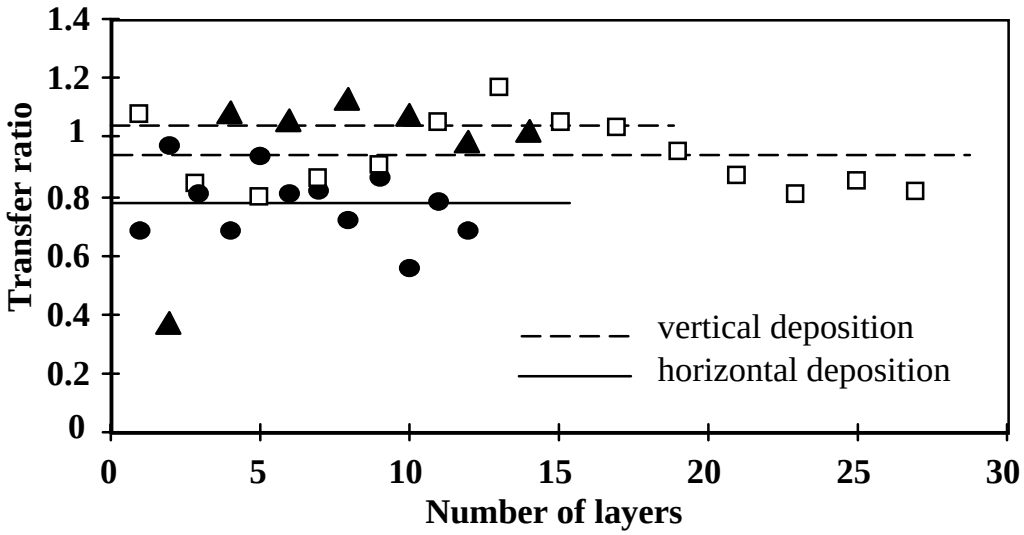

Figure 7. The deposition of CdC_{20} (❑) and CdC_{20}/1,1´-diarachidoylindigo (▲) mesasured with a SAW device [I,II] and the deposition of CdC_{20} measured with a QCM (●). The straight lines indicate the average transfer ratios.

4.1.2 Characterization with a surface plasmon resonance device

Information on the transferability of layers can also be obtained by using the SPR device (Fig. 8). The angular shift in the minima and in the position of the slope of the resonance curve with number of CdC_{22} layers deposited onto an Au and Pd coated glass slide corresponded to the theoretically calculated value [III], which indicates that the layers were reproducibly transferred (Fig. 8b). The position of the 'downward' slope of the SPR curve was most affected by the addition of layers [III]. In the experimental curves the depth of the SPR minima, however, shifted upwards with increasing number of layers [III]. The LB layers were treated as isotropic in the theoretical calculations, which is not necessarily the case. The discrepancy between theoretical and experimental curves can be associated with optical losses in the film, which in fact most probably was due to imperfections in the LB layer.

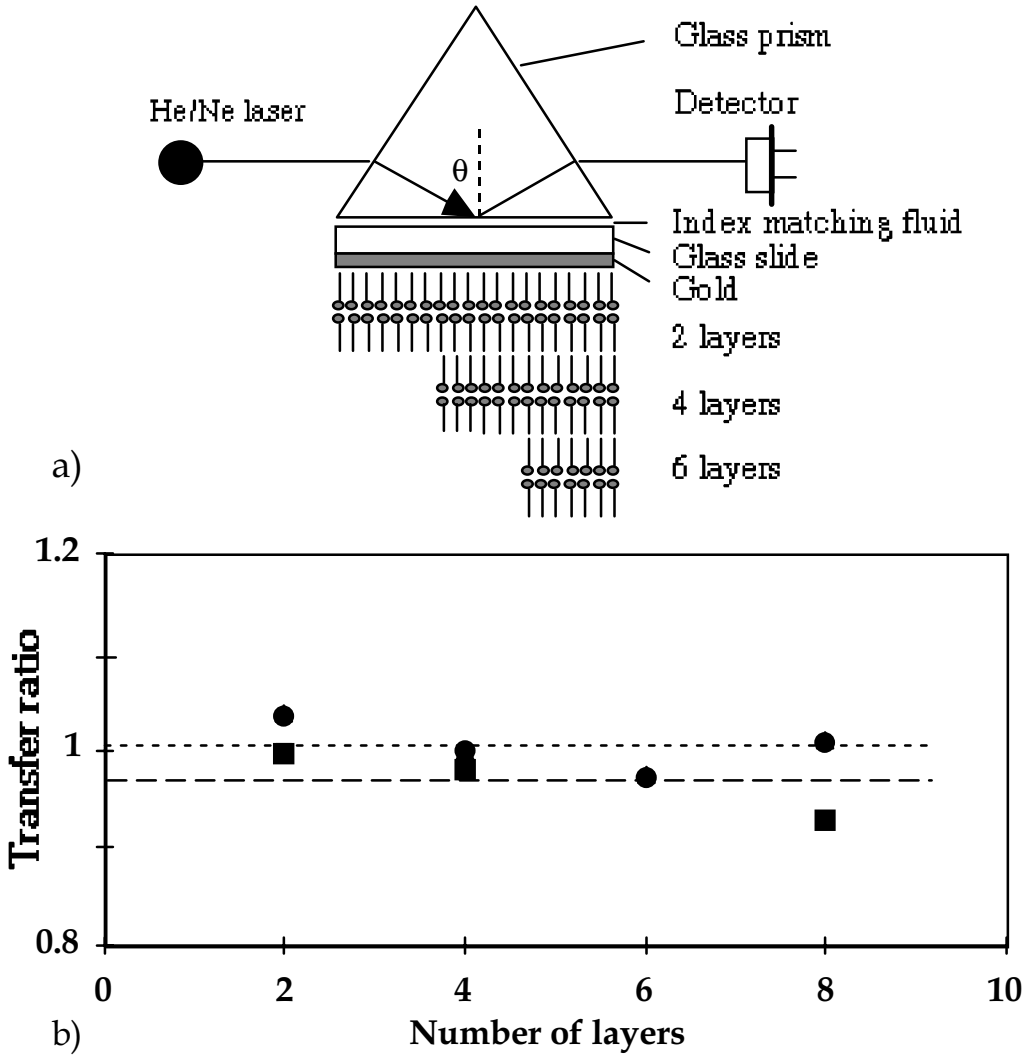

Figure 8. a) Schematic view of monolayers of CdC_{22} built up on an Au slide and b) the transfer ratio versus number of layers. The transfer ratio was obtained as a ratio between the measured and calculated angular shift in the position of the slope of the SPR resonance curve for CdC_{22} on Au (---●---) and Pd (– –■– –). The straight lines indicate the average transfer ratios.

It should be noted, that gold surfaces are readily contaminated because of their very high surface energy [101]. If the deposition was performed on Au slides freshly prepared, transfer on the downward movement of the slide was poor.

4.1.3 Topographic imaging

AFM commonly reveals defects in LB films with sizes ranging from a few square nanometers to several square microns [80,102-105] and with a bilayer depth [106]. The number and depth of the holes observed in CdC_{20} layers deposited on

glass [Fig. 2 Paper V] turned out to be dependent on how the slide was positioned in relation to the compressing barrier. The multilayer structure was much more homogeneous if the slide was positioned parallel, instead of perpendicular to the compressing barrier during monolayer transfer. The same conclusion was drawn from scanning tunnelling microscopy of phospholipid layers deposited on pyrolytic graphite [107]. Daniel et al. [108,109] has shown that the surface flow of spread monolayers influences film morphology. The morphology of the film varied across the slide and if the slide was positioned parallel to the barrier the crystallites were smaller on the side oriented towards the barrier than on the opposite side [109]. Daniel et al. [109] hereby draw the conclusion that the slide should be oriented parallel to the compressing barrier. In our studies, we only used the side oriented towards the barrier [V].

Monolayers of barium arachidate have been found to possess small holes when transferred horizontally [110], whereas multilayers of CdC_{20} and arachidic acid have a non-uniform structure [V, 110]. Seki et al. [111] proposed a simultaneous flopping at the air-water interface on horizontal deposition or a slow flopping relaxation due to exposure of the hydrophilic groups to air. Reorganization of molecules, starting at holes in the films, would lead to a non-uniform film structure. Holes in multilayers grow with age [112] and several groups have reported on the reorganization of molecules in LB films [80,106,113]. Fatty acid films deposited as X-type are identical to Y-type films. Models have been proposed on overturning molecules underwater, while others suggest that this process takes place as the monolayer is transferred [114,115]. The influence of the transfer mode on the film structure was further discussed in Paper V.

4.2 LAYER FORMATION BY SPREADING FROM VESICLES

Our purpose was initially to embed ALDH into lipid layers by fusion from vesicles [V]. ALDH can easily be incorporated into vesicles with remaining functional activity [18]. The preparation and storing of the vesicle suspensions, however, turned out to be crucial, as problems arose when we had to store the vesicle suspension frozen in order to maintain the activity of the enzyme. The stored vesicle suspensions will be referred to as aged vesicles.

Spreading of DMPC vesicle suspensions onto the air-liquid interface resulted in compression isotherms similar in shape to that of pure DMPC spread from a chloroform solution. Round domains of unfused vesicles were, however, observed by AFM on films spread from aged DMPC and DMPC/ALDH vesicles [V]. ALDH-containing vesicles gave films with domains clearly bigger than those of pure DMPC films. The real size of the domains was influenced by a convolution effect arising from the size of the tip. The exact curvature radius of the tip was not

known, but taken to be 50 nm [88]. The domains of the DMPC films could then be estimated to have a diameter of about 10-50 nm, whereas films spread from DMPC/ALDH vesicle suspenions had domains with an object diameter of about 220-900 nm [V]. The size of the domains did not depend on deposition mode. The density of the domains was, however, much less if the film was vertically transferred.

Large features of unfused vesicles have also been observed by Fare et al. [30] and found to adhere to mica, when spread directly onto the surface from an aged suspension [116]. Moreover, vesicles prepared by sonication fused directly onto solid supports forming membranes thinner than vesicles frozen and thawed several times [117]. It seems apparent that the freezing procedure made the vesicles more stable and maybe also led to the formation of aggregates. That was probably the reason the aged vesicles did not open to form a monolayer [V].

Films spread from freshly prepared vesicle suspensions could, on the downward movement be transferred onto hydrophobic glass slides with a transfer ratio of 0.75, whereas the slides emerged wet on the upward movement, indicating that no additional layer was transferred (Table 4). The horizontal deposition onto hydrophobic slides was successful, whereas nothing stuck to hydrophilic slides, which emerged completely wet.

Table 4. Transfer ratios of a monolayer spread from a freshly prepared vesicle suspension onto 9 layers of CdC_{20}.

	τ Vertical deposition	τ Horizontal deposition	
down	0.75		
up	0.05		
		0.86	QCM
	0.77	0.79	AFM

QCM ratios were obtained from the amount of layer transferred to that theoretically calculated and the AFM histograms gave the percentage layer coverage [V].

Holes with a depth of about 3 nm, corresponding to a lipid monolayer, could be observed on AFM images transferred by horizontal and vertical deposition [V]. The size of the holes in films transferred horizontally was clearly bigger, but the

density of the holes was lower than those in vertically transferred films [Fig.4 in Paper V]. A small number of holes corresponding to a bilayer thickness could also be imaged. These were probably due to the underlying CdC_{20} layer and the holes therein. Transfer of the lipid film onto the QCM gave an increase in surface density of 190 ng/cm^2, which corresponded to a transfer ratio of 0.86. The monolayer coverage in the AFM image agreed with the transfer ratios (Table 4). Phospholipid layers are normally difficult to deposit. DPPC can only be deposited as a single layer and there appears, furthermore, to be water present in the film [118]. The appearance of holes could thus partly be due to a drying of the film. Individual protein molecules were not identifiable on the images, probably because of the low concentration and hence insufficient incorporation into the layers.

Structural defects in the vesicle membrane may have initiated the fusion. Heyn et al. [26] have reported that unilamellar vesicles form uniform monolayers, whereas multilamellar vesicles form monolayers from the outer bilayer with the residue remaining attached. The fusion process was described by a bilayer-monolayer exchange model [22,26].

4.3 ANTIBODY LAYER FORMATION AT THE AIR-WATER INTERFACE

Some preliminary studies were performed on spreading anti-CRP directly onto the air-water interface in order to evaluate the film formation behaviour of the antibody [IV]. Anti-CRP formed a liquid-expanded monolayer (Fig. 9) with an isotherm similar in shape to the antibody studied by Alhuwalia et al. [35,36]. A transition between two ‘phases’ was indicated by the presence of an isopiestic point [36]. This transition occurred at a surface pressure between 10 - 15 mN/m for anti-CRP.

The antibody molecule can be represented by a disc with a diameter, d, of about 15 nm and a thickness, t, of about 3 nm [119] (Fig. 10a). If the molecules were standing end-on, a dense packing of antibodies would give a surface density of about $\Lambda = 0.75$ µg/cm^2, and if they were oriented in a side-on manner, the surface density would be about $\Lambda = 0.15$ µg/cm^2 [IV]. The anti-CRP film could be transferred onto the QCM with a surface density of 0.33 µg/cm^2 (Fig.9). This amount corresponds to about 40% of a monolayer coverage with the antibodies in an end-on position. It is, however, likely that the antibodies take up either a slanted orientation or have a random distribution in the film (Fig. 10b). Ahluwalia et al. [36] transferred films with surface densities ranging from 0.2 - 0.5 µg/cm^2 at pressures below the transition point, indicating antibodies with a similar orientation as anti-CRP. The quantity of antibodies transferred depends both on the surface pressure and on the pre-treatment of the slide [36-38]. Anti-CRP was, however, rinsed away from the QCM with the standard buffer solution, which was

of high ionic strength, but not with water. The first layer seemed to remain on the QCM, but it was difficult to discriminate between specific and non-specific adsorption because of the desorption. A total protein amount of about 0.3 µg/cm^2 adsorbed onto the layer [IV].

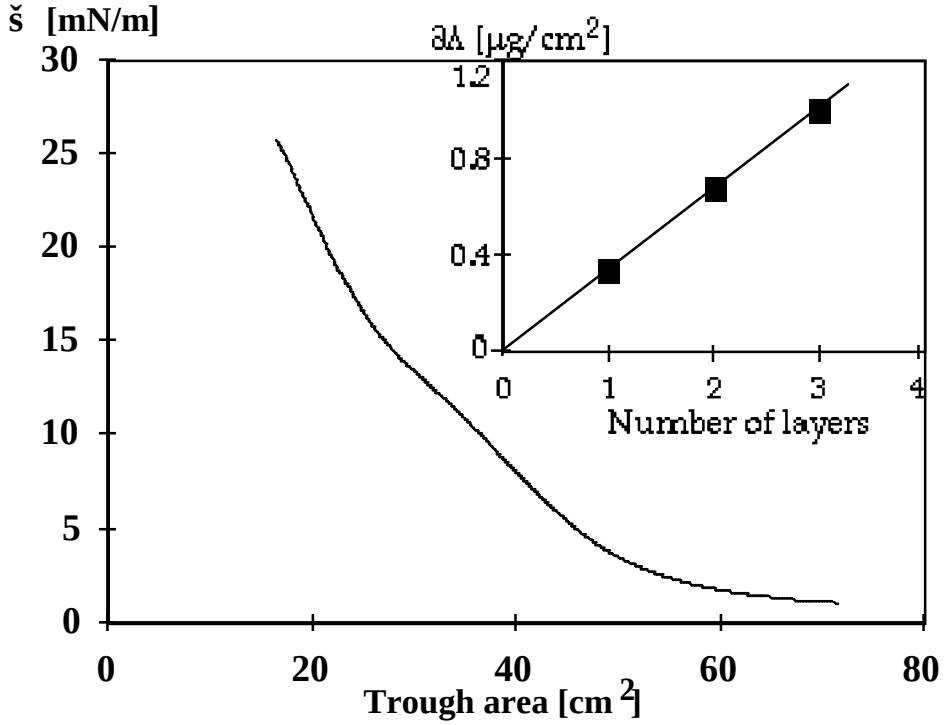

Figure 9 The surface pressure versus trough area curve for compression of anti-CRP spread onto a 1 mM $CaCl_2$ subphase of pH 8.2 (the isoelectric point of the antibody). The inset shows the increase in mass on deposition of the layer onto a QCM at a surface pressure of 10 mN/m.

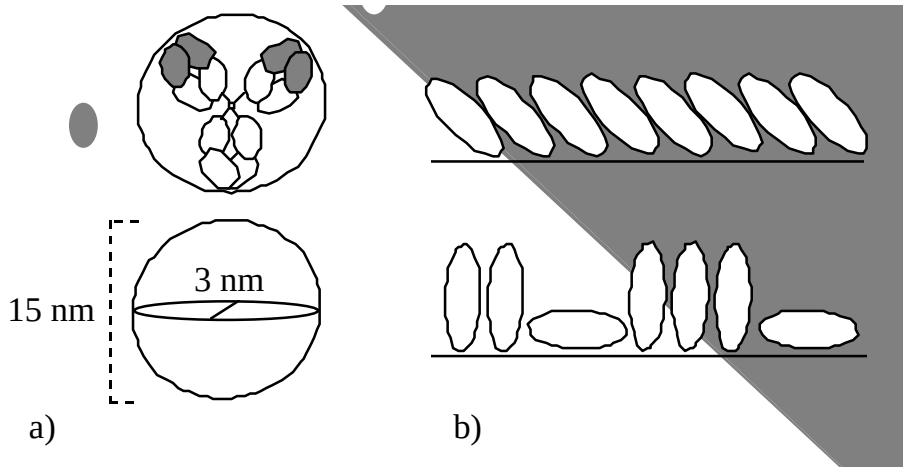

Figure 10 a) The antibody molecule will approximately take the form of a disc with a diameter of 15 nm and a thickness of 3 nm. b) The anti-CRP molecules seemed to have a slanted orientation (above) or a random distribution (below) with a surface density of 0.33 µg/cm^2.

4.4 ADSORPTION OF ANTIBODIES ONTO MONOLAYERS

Information on the binding of anti-CRP onto monolayers of C_{20}, ODA and DMPC/DMPE was obtained from relaxation studies and surface pressure - area isotherms [IV]. Anti-CRP was allowed to interact with ODA at a pH of 10, where ODA shows maximum monolayer stability [9]. C_{20} was almost half-ionised and the phospholipid monolayer was zwitterionic [IV]. When the ODA monolayer was held at a ¹ of 10 mNm^{-1}, antibodies adsorbed and/or penetrated into the layer as observed by an increase in surface area. The increase in surface area was dependent on the packing of the film and was not observed over a pressure of 15 mNm^{-1} [IV]. Incorporation of proteins has been found to stabilize monolayers at the air-water interface [59,120,IV].

The antibodies had an expanding and fluidizing effect upon the monolayers - an effect that was concentration dependent [IV]. The surface area of the ODA monolayer increased with increasing anti-CRP concentration in the subphase up to an antibody concentration of about 2.4 µg/ml. This was also observed from the relaxation studies, which showed a concentration dependence at low surface pressure [IV]. The increase in surface area of C_{20} was higher than that of ODA (Table 5). The interaction of antibodies with the DMPC/DMPE matrix, on the other hand, showed the same percentage by molecular area increase as ODA. Anti-CRP could not, however, be transferred onto the QCM from the DMPC/DMPE matrix and the relative amount transferred was lower for C_{20} than for ODA, although the area increase was almost twice as great (Table 5). The table also shows that a higher number of lipid-tagged single-chain antibodies could be incorporated into the lipid monolayers [IV, VII].

Table 5. Surface characteristics of anti-CRP and Ox lpp-scFv, when embedded into different monolayer matrices [IV, VI, VII].

Matrix	_A(%)* anti-CRP	_Λ(%) anti-CRP	_A(%)** Ox lpp-scFv	_Λ(%) Ox lpp-scFv	
C_{20}	27	20			[IV]
ODA	15	37			[IV]
DMPC/DMPE	15	-	35	36	[IV, VII]
DPPC/DPPE/DPPA			50	52	[VII]
DPPC/DPPE/DPPA/CHOL			60	25	[VII]

_A* is the increase in surface area obtained from the isotherm at a ¹=20mN/m and _A** is the increase at 30 mN/m. _Λ represents the surface density of antibodies transferred onto the QCM at the related pressures.

Ellipsometric data indicate that antibodies may take an upright position in the monolayer [59]. Nothing can, however, be concluded about the Fc-Fab_2 orientation from these measurements, although it was expected that the Fc fragment was oriented towards the monolayer, because of the hydrophobicity of the fragment. The interaction of anti-CRP with ODA was further discussed in Paper IV.

In Paper IV we also discussed the adsorption of protein onto the layers. BSA was used to block non-specific binding sites - a standard procedure in immunoassay. An amount of 3 $\mu g/cm^2$ of BSA adsorbed onto the uncoated QCM within 5 minutes. The total amount of protein adsorbed onto the ODA and ODA/anti-CRP layer was 1.2 $\mu g/cm^2$ and 1.5 $\mu g/cm^2$, respectively. We thereof draw the conclusion that about 0.3 $\mu g/cm^2$ was due to a specific binding of antigen and that about 1 ± 0.5 of a CRP monolayer seemed to be bound, if the reproducibility was taken into account [IV].

I would, however, like to address attention on the kinetics of the binding. Fig. 11 shows that the adsorption of protein from solutions containing BSA and increasing concentrations of CRP onto layers of CdC_{20} and ODA differed from that of C_{20}/anti-CRP. The binding of proteins to CdC_{20} and ODA reached an equilibrium within 30 minutes, whereas a plateau value was reached within 10 minutes for C_{20}/anti-CRP. The plateau value of the C_{20}/anti-CRP layer indicates that the non-specific binding sites were blocked and, furthermore, that low antigen concentrations could not be discriminated from the non-specific adsorption of BSA. The non-specific binding was similar to that onto the uncoated QCM. An abrupt increase in surface mass density at a higher CRP concentration, on the other hand, suggests that a specific interaction between antibodies in the C_{20}/anti-CRP layer and antigen took place.

The non-specific adsorption was much lower to antibody-containing layers than to the lipid layers (Table 6). The high binding of protein to CdC_{20} and ODA was probably due to a non-homogeneous deposition of the layers, with binding to holes and cracks in the film. The layers were horizontally transferred and the binding was, moreover, measured in air. AFM images showed that CdC_{20} layers horizontally transferred are very non-homogeneous [V]. It is known that the binding of BSA is strong to hydrophobic surfaces [121,122]. The binding was highest to CdC_{20} (Table 6). If Y-type CdC_{20} layers were transferred horizontally according to Lee et al. [14], only 0.4 $\mu g/cm^2$ BSA was adsorbed. This seems to confirm the earlier discussed reorganization of X-type CdC_{20} layers [V], leading to cracks and holes in the film and thus to a high adsorption of protein.

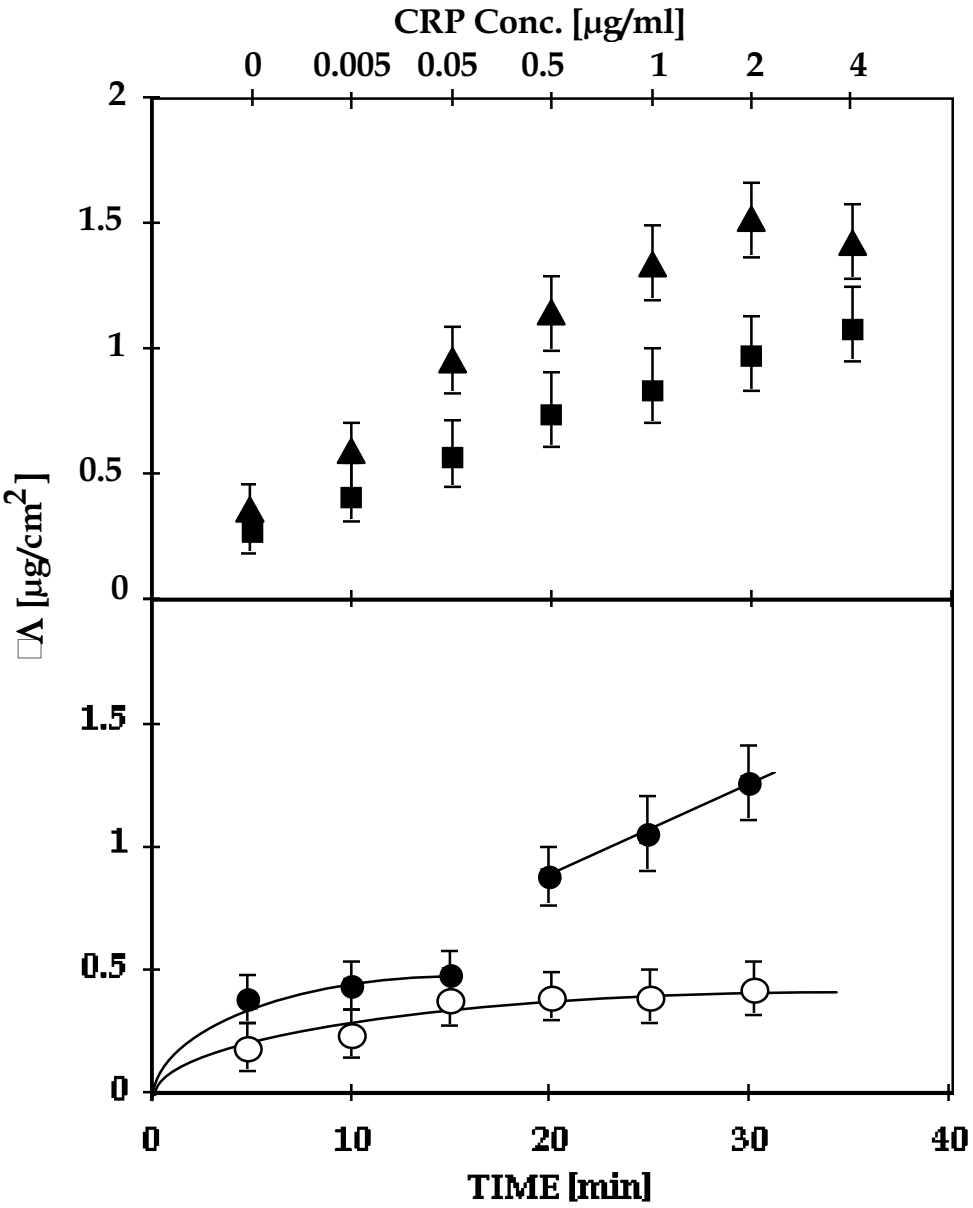

Figure 11. Adsorption of 0.5 mg/ml BSA and increasing concentration of CRP onto an uncoated QCM (○) and onto a QCM deposited with a monolayer of C_{20}/anti-CRP (●), a monolayer of ODA (■) and 12 layers of CdC_{20} (▲).

Table 6. Total amount of protein adsorbed onto different layers horizontally transferred onto the QCM during 5 minutes.

Layers	_Λ[µg/cm^2] BSA	CRP
CdC_{20}	1.5	
C_{20}/anti-CRP	0.5	0.8
ODA	1.2	
ODA/anti-CRP	0.3	1.2
DMPC	0.8	

The concentration dependence on the interaction of CRP with anti-CRP containing layers is shown in Fig. 12. The specific interaction was higher to the ODA/anti-CRP layer than to the C_{20}/anti-CRP layer (Table 6). This could be expected due to the higher amount of antibody transferred with ODA (Table 5). The high amount of antigen, however, indicated that CRP took up more than a monolayer. A monolayer of CRP (Stokes radius of 4.9 nm) would have a surface density of 0.3 µg/cm^2. A possible explanation is that CRP formed aggregates. In fact, CRP may stack to form decamers [95]. Specific binding of IgG (Stokes radius of 5.6 nm) with surface densities ranging from 1.3 to 1.7 µg/cm^2 has also been reported [123,124].

If the QCM was deposited with a new layer of ODA/anti-CRP in between every interaction with protein, the saturation was obtained at about 0.8 µg/cm^2 (Fig. 12). Although the interaction time (1 minute) was shorter, there seems to be some difference in the binding compared to the aforementioned. Aggregation of CRP could explain the adsorption of a higher amount of CRP onto layers that were allowed to interact with the protein solutions several times instead of only once. Moreover, a poor reproducibility of the measurements could be due to aggregation of the antigen, but also due to a random orientation of the antibodies in the layer. The attempted molecular organisation is shown in Fig. 13.

The antibody-antigen interaction should be confirmed by an independent method. This could be achieved by using labelled antibodies and standard immunoassay. This was, however, not possible within the scope of the project. The immunological measurements should, moreover, be performed in a liquid environment in order to avoid side effects caused by drying the layer. The QCM available at that time did, however, not resonate in liquid.

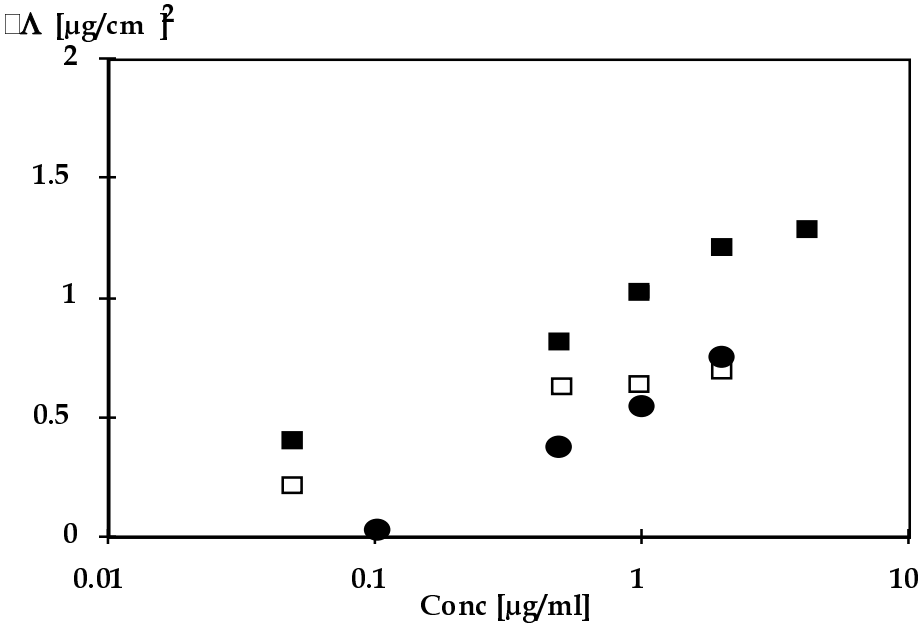

Figure 12. Interaction of CRP with anti-CRP layers transferred onto the QCM expressed as a change in mass vs log concentration of antigen. Increasing concentrations of CRP were allowed to interact with ODA/anti-CRP (■) and C_{20}/anti-CRP (●) for 5 minutes. (❒) represents the interaction of CRP for 1 minute with separate monolayers of ODA/anti-CRP. The non-specific adsorption of BSA has been reduced.

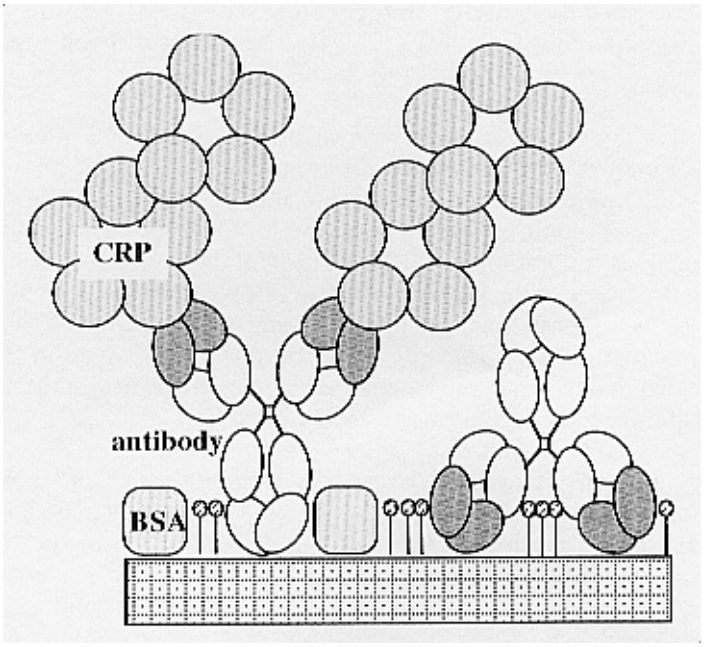

Figure 13. A schematic view of BSA and CRP binding to a layer incorporating whole antibodies produced according to the scheme in Paper IV. CRP is a cyclic pentamer that may aggregate to form decamers.

4.5 INCORPORATION OF SINGLE-CHAIN ANTIBODIES INTO DIFFERENT LIPID MATRICES

The incorporation of different amounts of single-chain antibodies into various preformed lipid monolayers was investigated by surface pressure - area isotherms and AFM [VI, VII]. Hydrophobic lipid-tags of about 2 kD [98] were thought to enable anchoring of the antibodies into the lipid layer. The molecular surface area increased on addition of Ox lpp-scFv to reach a saturation level that was dependent on the lipid matrix (Table 5) [VI, VII]. The mean molecular area of Ox lpp-scFv was estimated under the assumption that the antibodies remained at the interface and that the components were ideally mixed [I]. A value quite close to the theoretical surface area for an antibody fragment (3x4 nm^2) was obtained for the DPPC/DPPE/DPPA and DPPC/DPPE/DPPA/CHOL matrix, whereas the antibody incorporated into the DMPC/DMPE matrix gave a molecular surface area of about 7 nm^2.

The antibodies were segregated into protein-rich domains, which were smaller and more homogeneously distributed if DPPC/DPPE/DPPA was used as a layer matrix, instead of DMPC/DMPE [VII]. The diameter of the domains in the DMPC/DMPE matrix imaged in air was about 12 nm, if the convolution effect between the tip and the domains was taken into account [VI]. A mean height of about 6.5 nm corresponds fairly well to the expected length of the lipid-tagged antibody fragment [VI, VII]. These findings are similar to those of Heckl et al. [125], who reported that membrane proteins formed aggregates when incorporated into lipid monolayers. When the film was stored in buffer for some days before imaging, the film most probably underwent some reorganization or peeling [VII]. Height images revealed that the film had become quite rough and non-homogeneous. Storage of the films in buffer for one week showed that the size and the number of the holes further increased. Typical characteristics of the underlying CdC_{20} layers became clearly visible in the image. Imaging of the DPPC/DPPE/DPPA/Ox lpp-scFv after storage in buffer for one week indicated a much higher stability of this film, with only a partial peeling off the lipid layer. The domains in the DPPC/DPPE/DPPA matrix had a height of 3 nm and they appeared as dark areas of low friction. The domains were assumed to consist of single-chain antibodies, protruding from the layer, as the height corresponded well to a single-chain antibody. Larger domains of high friction were also imaged on both matrices, but the origin of them is not known.

Non-specific adsorption of BSA to the layers caused a shift in the SPR intensity, a shift that was further increased when the layer interacted with antigen, if Ox lpp-scFv had been incorporated into the film [VI, VII]. The intensity change was dependent on the concentration of $Ox_{16}BSA$, and was higher for DPPC/DPPE/DPPA/Ox lpp-scFv than for DMPC/DMPE/Ox lpp-scFv. This can

be explained both by a higher incorporation of antibody and a better transfer ratio. The binding of antigen could be detected in a concentration range of 0.1 - 100 µg/ml [VII].

The increase in molecular area of the DPPC/DPPE/DPPA/CHOL matrix on the incorporation of antibodies was the highest of the matrices studied (Table 5), but a poor transfer ratio led to a high non-specific adsorption of protein and subsequently to a low specific binding (Table 7). Holes in the layer act as non-specific adsorption sites and BSA may have interacted with the hydrophobic chains of the layer. The interaction of Ox_{16}BSA with the membrane was, in addition, influenced by the low incorporation of single-chain antibodies. The transfer ratio also affected the adsorption of BSA onto the DMPC/DMPE/Ox lpp-scFv layer. The amount of non-specific and specific binding was almost equal. The non-specific binding of BSA to the DPPC/DPPE/DPPA/Ox lpp-scFv layer was, on the other hand, very low. This could be explained by a good transfer ratio, giving a homogeneous layer with a minimum of defects. The highest specific interaction was obtained with DPPC/DPPE/DPPA/Ox lpp-scFv (Table 7) [VII]. The attempted molecular arrangement is shown in Figure 14.

Table 7. Relative amounts of specific binding of Ox_{16}BSA onto lipid layers incorporating Ox lpp-scFv measured with the SPR [VI, VII].

Lipid matrix	Specific binding (%) Ox_{16}BSA
DMPC/DMPE	45
DPPC/DPPE/DPPA	85
DPPC/DPPE/DPPA/CHOL	15

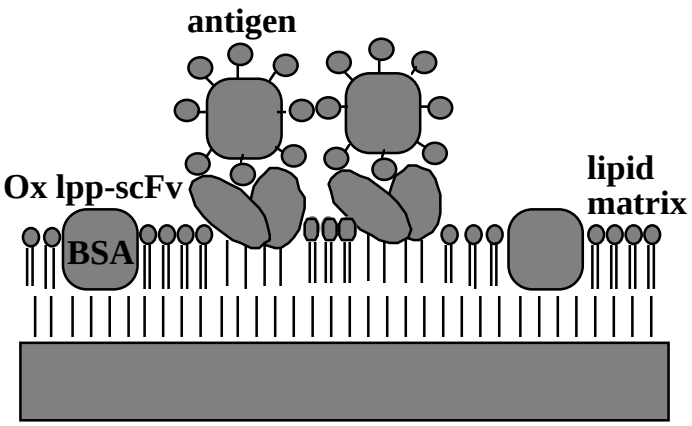

Figure 14. A schematic view of BSA and antigen-binding to a layer incorporating lipid-tagged single-chain antibodies. The layer was produced according to the scheme in Papers VI and VII.

5 CONCLUSIONS

This work was concentrated on the immobilization of proteins onto solid surfaces with the ultimate goal to contribute to the development of biosensors.

It turned out to be of utmost importance that the layer working as a solid support for the protein film should be defect-free, in order to minimise non-specific binding to cracks and holes in the layer. It was found that the solid slide should be positioned parallel to the compressing barrier when monolayers were vertically transferred, in order to obtain a more uniform LB film. Horizontal deposition of Cd arachidate, on the other hand, led to non-homogeneous layers. Piezoelectric devices could easily be used to monitor the yield of monolayer transfer.

Unilamellar vesicles were made to fuse at the air-water interface to form a monolayer. Additional studies are, however, needed in order to incorporate membrane proteins into these monolayers. Aged vesicles were stable and did not fuse, but they formed large domains.

Antibodies of the C-reactive protein, CRP, may be spread onto the air-water interface to form a monolayer. Anti-CRP could, moreover, be adsorbed onto various monolayers at the air-water interface in a concentration-dependent manner. Transfer of the antibodies onto a solid support was dependent on the monolayer matrix. Non-specific adsorption of protein was lower to the antibody-containing layer than to the pure monolayer. There seemed to be a specific binding of CRP to the layer in a concentration range of 0.1 - 5 µg/ml. The complex formation should, however, be complemented by standard immunoassay.

On the other hand, in order to orient antibodies in the layer a biosynthetically lipid-tagged single-chain antibody had to be used. Incorporation of the antibody fragment into various preformed lipid monolayers at the air-water interface was demonstrated. Atomic force microscopy revealed that protein-enriched domains were formed. The stability of the lipid layer in aqueous solution was poor, although antibodies seemed to have a stabilizing effect on the layer. Further research is needed to obtain a more homogeneous distribution of antibodies in the film and to increase the stability of the layer. Surface plasmon resonance was successfully employed to determine the antibody-antigen complex formation.

REFERENCES

1. Mattiasson, B. 1984. Immunochemical assays for process control: potentials and limitations. Trends in Analytical Chemistry 3, pp. 245 - 250.

2. Hall, E. 1992. Overview of biosensors. In: Edelman, D.G. and Wang, J. (eds.). Biosensors and Chemical Sensors. Am Chem. Soc., Washington. Pp. 1-14.

3. Andrade, J.D. 1985. Surface and Interface Aspects of Biomedical Polymers. Vol. 2. Plenum Press, New York. 347 p.

4. Kochev, V. and Filljov, K. 1992. From 'bulk' to 'interfacial' types of sensors. Sens. Actuators B 8, pp. 73 - 78.

5. Blodgett, K. 1935. Films built up depositing successive monomolecular layers on a solid surface. J. Am. Chem. Soc. 57, pp. 1007 - 1022.

6. Kuhn, H., Möbius, D. and Bücher, H. 1972. Spectroscopy of monolayer assemblies. In: Weissberger, A. and Rossiter, B. (eds.). Physical Methods of Chemistry. Part IIIB. Wiley, New York. Pp. 577 -702.

7. Gaines, G.L., Jr. 1966. Insoluble Monolayers at Liquid-Gas Interfaces. Wiley-Interscience, New York. 300 p.

8. Roberts, G. 1990. Langmuir-Blodgett films. Plenum Press, New York. 425 p.

9. Binks, B.P. 1991. Insoluble monolayers of weakly ionising low molar mass materials and their deposition to form Langmuir-Blodgett multilayers. Adv. Colloid Interface Sci. 34, pp. 343 - 432.

10. Peltonen, J., Linden. M., Fagerholm, H., Györvary, E. and Eriksson, F. 1994. The influence of multivalent salts on the processability of a stearic acid monolayer: a stability, electron spectroscopy for chemical analysis and atomic force microscopy study. Thin Solid Films 242, pp. 88 - 91.

11. Langmuir, I., Schaefer, V.K. and Sobotka, H. 1937. Multilayers of sterols and adsorption of digitonin by deposited monolayers. J. Am. Chem. Soc. 59, pp. 1751 - 1759.

12. Langmuir, I. and Schaefer, V.J. 1938. Activities of urease and pepsin monolayers. J. Am. Chem. Soc. 60, pp. 1351 - 1360.

13. Kawaguchi, T., Nakahara, H. and Fukuda, K. 1985. Monomolecular and multimolecular films of cellulose esters with various alkyl chains. Thin Solid Films 133, pp. 29 - 38.

14. Lee, S., Virtanen, J.A., Virtanen, S.A. and Penner, R.M. 1992. Assembly of fatty acid bilayers on hydrophobic substrates using a horizontal deposition procedure. Langmuir 8, pp. 1243 - 1246.

15. Singer, S.N. and Nicolson, G.L. 1972. The fluid mosaic model of the structure of cell membranes. Science 175, pp. 720 - 731.

16. Chapman, D., 1993. Biomembranes and new hemocompatible materials. Langmuir 9, pp. 39 - 45.

17. New, R.R.C. 1990. Liposomes a Practical Approach. Oxford University Press. 301 p.

18. Smolander, M., Buchert, J. and Viikari, L. 1993. Large-scale applicable purification and characterization of a membrane-bound PQQ-dependent aldose dehydrogenase. J. Biotech. 29, pp. 287 - 297.

19. Hope, M.J., Bally, M.B., Webb, G. and Cullis, P.R. 1985. Production of large unilamellar vesicles by a rapid extrusion procedure. Characterization of size distribution, trapped volume and ability to maintain a membrane potential. Biochim. Biophys. Acta 812, pp. 55 - 65.

20. Locascio-Brown, L., Plant, A.L., Chesler, R., Kroll, M., Ruddel, M. and Durst, R.A. 1993. Liposome-based flow-injection immunassay for determining theophylline in serum. Clin. Chem. 39, pp. 386 - 391.

21. Verger, R. and Pattus, F. 1976. Spreading of membranes at the air/water interface. Chemistry and Physics of Lipids 16, pp. 285 - 291.

22. Pattus, F., Desnuelle, P. and Verger, R. 1978. Spreading of liposomes at the air/water interface. Biochim. Biophys. Acta 507, pp. 62 - 70.

23. Pattus, F., Piovant, M.C.L., Lazdunski, C.J., Desnuelle, P. and Verger, R. 1978. Spreading of biomembranes at the air/water interface. Biochim. Biophys. Acta 507, pp. 71 - 82.

24. Schindler, H. 1979. Exchange and interactions between lipid layers at the surface of a liposome solution. Biochim. Biophys. Acta 555, pp. 316 - 336.

25. Salesse, Ch., Durcharme, D. and Leblanc, R.M. 1987. Direct evidence for the formation of a monolayer from a bilayer-An ellipsometric study at the nitrogen-water interface. Biophys. J. 52, pp. 351 - 352.

26. Heyn, S.P., Egger, M., Gaub, H.E. 1990. Lipid and lipid-protein monolayers spread from a vesicle suspension: a microfluorescence film balance study. J. Phys. Chem. 94, pp. 5073 - 5078.

27. Fischer, B., Heyn, S.P., Egger, M. and Gaub, H.E. 1993. Antigen binding to a pattern of lipid-anchored antibody binding sites measured by surface plasmon microscopy. Langmuir 9, pp. 136 - 140.

28. Egger, M., Heyn, S.P. and Gaub, H. E. 1990. Two-dimensional recognition pattern of lipid-anchored fab´ fragments. Biophys. J. 57, pp. 669 - 673.

29. Belorgey, O., Tchoreloff, P., Benattar, J.J. and Proust, J.E. 1991. An X-ray reflectivity investigation of a deposited layer of the natural lung surfactant. J. Colloid Interface Sci. 146, pp. 373 - 781.

30. Fare, T.L., Palmer, C.A., Silvestre, C.G., Cribbs, D.H., Turner, D.C., Brandow, S.L. and Gaber, B.P. 1992. Langmuir-Blodgett studies and atomic force microscope images of nicotinic acetylcholine receptor films. Langmuir 8, pp. 3116 - 3121.

31. Panaiotov, I., Proust, J. E., Raneva, V. and Ivanova, Tz. 1994. Kinetics of spreading at the air-water interface of dioleoylphosphatidylcholine liposomes influenced by photodynamic lipid peroxidation. Thin Solid Films 244, pp. 845 - 851.

32. Kalb, E., Frey, S. and Tamm, L.K. 1992. Formation of supported planar bilayers by fusion of vesicles to supported phospholipid monolayers. Biochim. Biophys. Acta 1103, pp. 307 - 316.

33. MacRitchie, F. 1978. Proteins at interfaces. Adv. Protein Chem. 32, pp. 283 - 326.

34. Sun, S., Ho-Si, P.-H. and Harrison, D.J. 1991. Preparation of active Langmuir-Blodgett films of glucose oxidase. Langmuir 7, pp. 727 - 737 and references herein.

35. Ahluwalia, A. Rossi, D.D., Monici, M. and Schirone, A. 1991. Thermodynamic study of Langmuir antibody films for application to immunosensors. Biosens. Bioelectronics 6, pp. 133 - 141.

36. Ahluwalia, A., Rossi, D.D., Rwastori, C., Schirone, A., Serra, G. 1992. A comparative study of protein immobilization techniques for optical immunosesnors. Biosens. Bioelectronics 7, pp. 207 - 214.

37. Turko, I.V., Yurkevich, I.S. and Chashchin, V.L. 1991. Langmuir-Blodgett films of immunoglobulin G for immunosensors. Thin Solid Films 205, pp. 113 - 116.

38. Dubrovsky, T.B., Demcheva, M.V., Savitsky, A.P., Mantrova, E.Y., Yaropolov, A.I., Savransky, V.V. and Belovolova, L.V. 1993. Fluorescent and phosphorescent study of Langmuir-Boldgett antibody films for application to immunosensors. Biosens. Bioelectronics 8, pp. 377 - 385.

39. Tronin, A., Dubrovsky, T., De Nitti, C., Gussoni, A., Erokin, V. and Nicoloni, C. 1994. Langmuir-Blodgett films of immunoglobulines IgG. Ellipsometric study of the deposition process and of immunological activity. Thin Solid Films 238, pp. 127 - 132.

40. Erokhin, V., Facci, P. and Nicoloni, C. 1995. Two-dimensional order and protein thermal stability: high temperature preservation of structure and function. Biosens. Bioelectronics 10, pp. 25 - 34.

41. Sriyudthsak, M., Yamagishi, H. and Moriizumi, T. 1988. Enzyme-immobilized Langmuir-Blodgett film for a biosensor. Thin Solid Films 160, pp. 463 - 469.

42. Furuno, T., Sasabe, H. and Ulmer, K.M. 1989. Binding of ferritin molecules to a charged polypeptide layer of poly-1-benzyl-L-histidine. Thin Solid Films 180, pp. 23 - 30.

43. Krull, U.J., Koilpillai, R.N., Rae, C.O. and Vandenberg, E.T. 1991. Electrostatic and structural alterations of lipid monolayers and bilayers by interaction with valinomycin and phloretin. Thin Solid Films 195, pp. 279 - 288.

44. Tomoaia-Cotisel, M. and Cadenhead, A.D. 1991. Interaction of procaine with stearic acid monolayers at the air/water interface. Langmuir 7, pp. 964 - 974.

45. Piepenstock, M. and Lösche, M. 1992. Steric and electrostatic aspects of antibody binding to hapten functionalized lipid monolayers. Thin Solid Films 210/211, pp. 793 - 795.

46. Sugawara, M., Sazawa, H.and Umezawa, Y. 1992. Effect of the membrane surface charge on the host-guest complex of valinomycin in a synthetic lipid monolayer at the air-water interface. Langmuir 8, pp. 609 - 612.

47. Ebara, Y. and Okahata, Y. 1993. In situ surface-detecting technique by using a quartz-crystal microbalance. Interaction behaviors of proteins onto a phospholipid monolayer at the air-water interface. Langmuir 9, pp. 574 - 576.

48. Fujiwara, I., Ohnishi, M. and Seto, J. 1992. Atomic force microscopy study of protein-incorporating Langmuir-Blodgett films. Langmuir 8, pp. 2219 - 2222.

49. Li, J.R., Cai, M., Chen, T.F. and Jiang, L. 1989. Enzyme electrodes with conductive polymer membranes and Langmuir-Blodgett films. Thin Solid Films 180, pp. 205 - 210.

50. Arisawa, S. and Yamamoto, R. 1992. Quantitiative characterization of enzymes adsorbed on to Langmuir-Blodgett films and the application to a urea sensor. Thin Solid Films 210/211, pp. 443 - 445.

51. Fiol, C., Valleton, J.M. Delpire, N., Barbey, G., Barraud, A. and Ruaudel-Teixier, A. 1992. Elaboration of a glucose biosensor based on Langmuir-Blodgett technology. Thin Solid Films 210/211, pp. 489 - 491.

52. Sameulson, L.A.,Kaplan, D.L., Lim, J.O., Kamath, M., Marx, K.A. and Tripathy, S.K. 1994. Molecular recognition between a biotinylated polythiophene copolymer and phycoerythrin utilizing the biotin-streptavidin interaction. Thin Solid Films 242, pp. 50 - 55.

53. Lee, S., Anzai, J. and Osa, T. 1993. Enzyme-modified Langmuir-Blodgett membranes in glucose electrodes based on avidin-biotin interaction. Sens. Actuators B 12, pp. 153 - 158.

54. Hoffmann, M., Müller, W., Ringsdorf, H., Rouke, A.M., Rump, E. and Suci, P.A. 1992. Molecular recognition in biotin-streptavidin systems and analogues at the air-water interface. Thin Solid Films 210/211, pp. 780 - 783.

55. Samuelson, L., Miller, P., Galatti, D., Marx, K.A., Kumar, J., Tripathy, S. and Kaplan, D. 1992. Langmuir-Blodgett films of streptavidin-conjugated phycoerythrin bound to biotinylated monolayers. Thin Solid Films 210/211, pp. 796 - 798.

56. Heckl, W.M., Thompson, M. and Möhwald, H. 1989. Fluorescence and electron microscopic study of lectin-polysaccharide and immunochemical aggregation at phospholipid Langmuir-Blodgett monolayers. Langmuir 5, pp. 390 - 394.

57. Barraud, A., Perrot, H., Billard, V., Martelet, C., Therasse, J. 1993. Study of immunoglobulin G thin layers obtained by Langmuir-Blodgett method: application to immunosensors. Biosens. Bioelectronics 8, pp. 39 - 48.

58. Pillet, L., Perez, H., Ruaudel-Teixier, A. and Barraud, A. 1994. Immunoglobulin immobilization by the Langmuir-Blodgett method. Thin Solid Films 244, pp. 857 - 859.

59. Wang, H., Brennan, J.D., Gene, A. and Krull, U.J. 1995. Assembly of antibodies in lipid membranes for biosensor development. Applied Biochem. Biotech. 53, pp. 163 - 181.

60. Andle, J.C. and Vetelino, J.F. 1994. Acoustic wave biosensors. Sens. Actuators A 44, pp. 167 - 176.

61. Sauerbrey, G. 1959. Verwendung von schwingquarzen zur wägung dünner schichten und zur mikrowägung. Z. Phys. 155, pp. 206 - 222.

62. Muramatsu, H.and Kimura, K. 1992. Quartz crystal detector for microrheological study and its application to phase transition phenomena of Langmuir-Blodgett films. Anal. Chem. 64, pp. 2502 - 2507.

63. Hauptmann, P. 1991. Resonant sensors and applications. Sens. Actuators A 25, pp. 371 - 377.

64. Muratsugu, M., Ohta, F., Miya, Y., Hosokawa, T., Kurosawa, S., Kamo, N. and Ikeda, H. 1993. Quartz crystal microbalance for the detection of microgram quantities of human serum albumin: Relationship between the frequency change and the mass of protein adsorbed. Anal . Chem. 65, pp. 2933 - 2937.

65. Petty, M.C. 1995. Gas sensing using thin organic films. Biosens. Bioelectronics 10, pp. 129-134.

66. Wohltjen, H. 1984. Mechanism of generation and design considerations for surface acoustic wave device vapour sensors. Sens. Actuators 5, pp. 307 - 325.

67. Wohltjen, H. and Dessy, R. 1979. Surface acoustic wave probe for chemical analysis. Anal. Chem. 51, pp. 1458 - 1475.

68. Vikholm, I. and Helle, H. 1992. Langmuir-Blodgett films of hexadecylvinylbenzyldimethylammonium chloride and their ozone sensitivity. Thin Solid Films 210/211, pp. 368 - 371.

69. Chang, S.-M. Ebert, B., Tamiya, E. and Karube, I. 1991. Development of chemical vapour sensor using SAW resonator oscillator incorporating odorant receptive LB films. Biosens. Bioelectr. 6, pp. 293 - 298.

70. Otto, A. 1968. Excitation of non-radiative surface plasma waves in silver by the method of frustrated total reflection. Z. Phys. 216, pp. 398 - 405.

71. Kretschmann, E. and Raether, H. 1971. The determination of optical constants of metal by excitation of surface plasmons. Z. Phys. 241, pp. 313 - 321.

72. Sadowski, J., Korhonen, I., and Peltonen, J. 1995. Characterization of thin films and their structures in surface plasmon resonance measurements. Optical Engineering 34, pp. 2581 - 2586.

73. Lekkala, J., Albers, M. and Sadowski, J.W. 1991. In: Proceedings of World Congress on Medical Physics and Biomedical Engineering. Kyoto, Japan, 7-12 July, 1991. P. 1054.

74. Lawrence,, C.R., Martin, A.S.and Sambles, J.S. 1992. Surface plasmon polariton studies of highly absorbing Langmuir-Blodgett films. Thin Solid Films 208 pp. 269 - 273.

75. Noe, L.J., Tonoaia-Cotisel, M., Casstevens, M. and Prasad, P.N. 1992. Characterization of Langmuir-Blodgett films of 3,4-didecyloxy-2,5-di(4-nitrophenylazomethine)thiophene. Thin Solid Films 208, pp. 274 - 279.

76. Morgan, H. and Tayor, D.M. 1992. A surface plasmon resonance immunosensor based on the streptavidin-biotin complex. Biosens. Bioelectronics 7, pp. 405 - 410.

77. Binnig, G., Quate, C.F. and Gerber, Ch. 1986. Atomic force microscope. Phys. Review Lett. 56, pp. 930 - 933.

78. Butt, H.-J., Downing, K.H. and Hansma, P.K. 1990. Imaging the membrane protein bacteriorhodopsin with the atomic force microscope. Biophys. J. 58, pp. 1473 - 1480.

79. Radmacher, M., Tillmann, R.W. and Gaub, H.E. 1992. From molecules to cells: Imaging soft samples with the atomic force microscope. Science 257, pp. 1900 - 1905 and references herein.

80. Schaper, A., Wolthaus, L., Möbius, D. and Jovin, T.M. 1993. Surface morphology and stability of Langmuir-Blodgett mono- and multilayers of saturated fatty acids by scanning force microscopy. Langmuir 9, pp. 2178 - 2184.

81. Zasadzinski, J.A.N., Helm., C.A., Longo, M.L., Weisenhorn, A.L., Gould, A.C. and Hansma, P.K. 1991. Atomic force microscopy of hydrated phosphatidylethanolamine bilayers. Biophys. J. 59, pp. 755 - 760.

82. Green, J.-B., McDermott, M.T., Porter, M.D. and Siperko, L.M. 1995. Nanometer-scale mapping of chemically distinct domains at well-defined organic interfaces using frictional force microscope. J., Phys.Chem. 99, pp. 10960 - 10965.

83. Hoh, J.H. and Engel, A. 1993. Friction effects on force measurements with an atomic force microscope. Langmuir 9, pp. 3310 - 3312.

84 Overney, R.M., Myer, E., Frommer, J., Brodbeck, D., Lüthi, R., Howald, 1L., Güntherodt, H.J., Fujihira, M., Takano, H. and Gotoh, Y. 1992. Friction measurements on phase-separated thin films with a modified atomic force microscope. Nature 359, pp. 133 - 135.

85. Marti, O., Colochero, J. and Mlynek, J. 1992. Friction and force on an atomic scale. Nato ASI Series E:235.

86. Schwartz, D.K., Garnaes, R., Viswanathan, R. and Zasadzinski, J.A.N. 1992. Surface order and stability of Langmuir-Blodgett films. Science 257, pp. 508 - 511.

87. Butt, H.-J., Guckenberger, R. and Rabe, J.P. 1992. Ouantitative scanning tunneling microscopy and scanning force microscopy of organic materials. Ultramicroscopy 46, pp. 375 - 393.

88. Hanley, S.J., Giasson, J., Revol, J.-F. and Gray, D.G. 1992. Atomic force microscopy of cellulose microfibrils: comparison with transmission electron microscopy. Polymer 33, pp. 4639 - 4642.

89. Kivinen, A., Vikholm, I. and Tarpila, S. 1994. A film balance study of the monolayer-forming properties of dietary phospholipids and the interaction with NSAIDs on the monolayers. Int. J. Pharm. 108, pp. 109 - 115.

90. Troughton, E.B., Bain, C.D., Whitesides, G.M., Nuzzo, R.G., Allara, D. and Porter, M.D. Monolayer films prepared by spontaneous self-assembly of symmetrical and unsymmetrical dialkyl sulfides from solution onto gold substrates: structure, properties, and reactivity of constituent functional groups. Langmuir 4, pp. 365 - 385.

91. Bain, C. D., Biebuyck, A. and Whitesides, G.M. 1989. Comparison of self-assembled monolayers on gold: coadsorption of thiols and disulfides. Langmuir 5, pp. 723 -727.

92 Burton, D.R. 1987. Structure and function of antibodies. In: Calabi, F. and Neuberger, M.S. (eds.). Molecular Genetics of Immunoglobulins. Elsevier, Amsterdam. Pp. 1 - 50.

93. Winter, G. and Milstein, C. 1991. Man-made antibodies. Nature 349, pp. 293 - 299.

94. Oliveira, E.B., Gotschlich, E.C. and Lui, T.-Y. 1979. Primary structure of human C-reactive protein. J. Biol. Chem. 254, pp. 489 - 502.

95. Osmand, A.P., Friedenson, B., Gewurz, H., Painter, R.H., Hofmann, T. and Shelton, E. 1977. Characterization of C-reactive protein and the complement C1t as homologous proteins displaying cyclic pentameric symmetry (pentraxins). Proc. Natl. Acad. Sci. USA 74, pp. 739 - 743.

96. Kusher, J. and Somerville, I.A. 1970. Estimation of the molecular size of C-reactive protein and C_X-reactive protein in serum. Biochim. Biophys. Acta 207, pp. 105 - 114.

97 Mazlam, M.Z. and Hodgson, H.J.F. 1994. Why measure C reactive protein? Gut 35, pp. 5 - 7.

98. Takkinen, K., Laukkanen, M.-L., Sizmann, D., Alfthan, K., Immonen, L., Vanne, M., Kaartinen, M., Knowles, K.C. and Teeri, T. 1991. An active single-chain antibody containing a cellulase linker domain is secreted by *Escherichia coli*. Protein Engineering 4, pp. 837 - 841.

99. Laukkanen, M.-L., Teeri, T. and Keinänen, K. 1993. Lipid-tagged antibodies: bacterial expression and characterization of lipoprotein single-chain antibody fusion protein. Protein Engineering 6, pp. 449 - 454.

100. Facci, P., Erokhin, V. and Nicolini, C. 1993. Nanogravimetric gauge for surface density measurements and deposition analysis of Langmuir-Blodgett films. Thin Solid Films 230, pp. 86 - 89.

101. Peterson, I.R., Veale, G. and Montgomery, C.M. 1986. The preparation of oleophilic surfaces for Langmuir-Blodgett deposition. J. Colloid Interface Sci. 109, pp. 527-530.

102. Hansma, H.G., Gould, S.A.C., Hansma, P.K., Gaub, H.E., Longo, M.L. and Zasadzinski., J.A.N. 1991. Imaging nanometer scale defects in Langmuir-Blodgett films with the atomic force microscope. Langmuir 7, pp. 1051 - 1054.

103. Viswanathan, R., Schwartz, D.K., Garnaes, J. and Zasadzinski, J.A.N. 1992. Atomic force microscopy imaging of substrate and pH effects on Langmuir-Blodgett monolayers. Langmuir 8, pp. 1603 - 1607.

104. Fuchs, H., Chi, L.F., Eng, L.M. and Graf, K. Defect structures of Langmuir-Blodgett films investigated by scanning force microscopy. Thin Solid Films 210/211, pp. 665 - 658.

105. Wolthaus, L.,Schaper, A., Möbius, D. and Jovin, T.M. 1994. Structural investigation of dipping lines in Langmuir-Blodgett films by scanning force microscopy. Thin Solid Films 242, pp. 170 -173.

106. Overney, R.M., Meyer, E., Frommer, J., Grünterodt, H.-J., Decher, G., Reibel, J. and Schling, U. 1993. A comparative atomic force microscopic study of liquid crystal films: transferred freely-suspended vs Langmuir-Blodgett. Morphology, lattice, and manipulation. Langmuir 9, pp. 341 - 346.

107. Niemi, H.E.-M., Ikonen, M., Levlin, J.M. and Lemmetyinen, H. 1993. Bacteriorhodopsin in Langmuir-Blodgett Films imaged with a scanning tunneling microscope. Langmuir 9, pp. 2436 - 2447.

108. Daniel, M.F. and Hart, J.T.T. 1985. Effect of surface flow on morphology of Langmuir-Blodgett films. J. Mol. Electron. 1, pp. 97 - 104.

109. Daniel, M.F., Dolphin, J.C., Grant, A.J., Kerr, K.E.N. and Smith, G.W. 1985. A trough for the fabrication of non-centrosymmetric Langmuir-Blodgett films. Thin Solid Films 133, pp. 235 - 242.

110. Matsumoto, M., Uyeda, N., Fujiyoshi, Y. and Aoyama, K. 1993. Dark-field electron microscopy of Langmuir-Boldgett films of fatty acids and their barium salts. Thin Solid Films 223, pp. 358 - 367.

111. Seki, T., Sakuragi, M., Kawanishi, Y., Suzuki, Y., Tamaki, T., Fukuda, R. and Ichimura, K. 1993. 'Command surfaces' of Langmuir-Blodgett films. Photoregulations of liquid crystal alignment by molecularly taylored surface azobenzene layers. Langmuir 9, pp. 211 - 218.

112. Chi, L-F., Eng, L.M., Graf, K. and Fuchs, H. 1992. Structure and stability of Langmuir-Blodgett films investigated by scanning force microscopy. Langmuir 8, pp. 2255 - 2261.

113. Schwartz, D.K., Viswanathan, R. and Zasadzinski, J.A.N. 1992. Reorganization and crystallite formation in Langmuir-Blodgett films, J. Phys. Chem., 96 pp. 10444 - 10447.

114. Peng, J.B., Ketterson, J.B., and Dutta, P. 1988. A study of the transition from Y- to X-type transfer during deposition of lead stearate and cadmium stearate Langmuir-Blodgatt films. Langmuir 4, pp. 1198 - 1202.

115. Hasmonay, H., Vincent, M. and Dupeyrat, M. 1980. Composition and transfer mechanism of Langmuir-Blodgett multilayers of stearates. Thin Solid Films 68, pp. 21 - 32.

116. Singh, S. and Keller, D.J. 1991. Atomic force microscopy of supported planar membrane bilayers. Biophys. J. 60, pp. 1401 - 1410.

117. Striebel, Ch., Brecht, A. and Gauglitz, G. 194. Characterization of biomembranes by spectral ellipsometry, surface plasmon resonance and interferometry with regard to biosensor application. Biosens. Bioelec. 9, pp. 139 - 146.

118. Taylor, D.M. and Mahboubian-Jones, M.G.B. 1982. The electrical properties of synthetic phospolipid Langmuir-Blodgett films. Thin Solid Films 87, pp. 167 - 179.

119. Silverton, E.W., Navia, M.A. and Davies, D.R. 1977. Three-dimensional structure of an intact human immunoglobulin. Proc. Nat. Acad. Sci. 74, pp. 5140 - 5144.

120. Krull, U.J., Brown, R.S., Vandenberg, E.T. and Heckl, W.M. 1991. Determination of the physical structure of biological materials at biosensor interfaces by techniques of increasing magnification from microscope to molecular scale. J. Electron Microscopy Technique 18, pp. 212 - 222.

121. Wright, L.L., Palmer, A.G. and Thompson, N.L. 1988. Inhomogeneous translational diffusion of antibodies specifically bound to phospholipid Langmuir-Blodgett films. Biophys. J. 54, pp. 463 - 470.

122. Gölander, C-G. and Kiss, E. 1988. Protein adsorption on functionalized and ESCA-characterized polymer films studied by ellipsometry. J. Colloid Int. Sci. 121, pp. 240 - 253.

123. Dubrovsky, T., Tronin, A., Dubrovskaya, S., Vakula, S. and Nicolini, C. 1995. Immunological activity of IgG Langmuir films oriented by protein A sublayer. Sens. Actuators B 23, pp. 1-7.

124. Erokhin, V., Facci, P., Dubrovsky, T., Tronin, A. and Nicolini, C. 1994. A new class of sensitive layers formed by modified Langmuir-Blodgett technique. In: Proceedings of the 5th Int. Meeting on Chemical Sensors. Rome 11-14 July 1994. Vol.1 pp.173 - 176

125. Heckl. W.M., Lösche, M. and Möwald, H. 1985. Langmuir-Boldgett films containing proteins of the photosynthetic process. Thin Solid Films 133, pp. 73-81.

ERRATA

Position	Error	Correction
Publ. III, page 441 at the last line	Cadmium behenate	cadmium behenate
Publ. V, page 114 end of second paragraph	110-450 nm	220-900 nm

Appendices of this publication are not included in the PDF version. Please order the printed version to get the complete publication (http://www.inf.vtt.fi/pdf/publications/1996)